A generalised model of electrical energy demand from small household appliances

A. Sancho-Tomás[a], M. Sumner[b], D. Robinson[c]

[a] *Faculty of Engineering, Department of Architecture and Built Environment, University of Nottingham, NG7 2RD, UK*
[b] *Faculty of Engineering, Department of Electrical Engineering, University of Nottingham, NG7 2RD, UK*
[c] *School of Architecture, University of Sheffield, S10 2TN, UK*

Abstract

Accurate forecasting of residential energy loads is highly influenced by the use of electrical appliances, which not only affect electrical energy use but also internal heat gains, which in turn affects thermal energy use. It is therefore important to accurately understand the characteristics of appliance use and to embed this understanding into predictive models to support load forecast and building design decisions. Bottom-up techniques that account for the variability in socio-demographic characteristics of the occupants and their behaviour patterns constitute a powerful tool to this end, and are potentially able to inform the design of Demand Side Management strategies in homes.

To this end, this paper presents a comparison of alternative strategies to stochastically model the temporal energy use of low-load appliances (meaning those whose annual energy share is individually small but significant when considered as a group). In particular, discrete-time Markov processes and survival analysis have been explored. Rigorous mathematical procedures, including cluster analysis, have been employed to identify a parsimonious strategy for the modelling of variations in energy demand over time of the four principle categories of small appliances: audio-visual, computing, kitchen and other small appliances. From this it is concluded that a model of the duration for which appliances survive in discrete states expressed as bins in fraction of maximum power demand performs best. This general solution may be integrated with relative ease with dynamic simulation programs, to complement existing models of relatively large load appliances for the comprehensive simulation of household appliance use.

Keywords: Electrical Appliances, Stochastic Modelling, Markov Chain, Occupant Behaviour, Demand Side Management, Cluster Algorithm, Residential Energy Use, Energy Planning

1. Introduction

In the UK approximately 20% of energy use in households is due to electrical appliances [1], and this proportion is higher in better insulated homes. Residential electrical appliance use has direct implications for local Low Voltage (LV) networks, the loads on them and their integrity; and indirect implications for thermal energy demands, since electrical energy is ultimately dissipated as heat, most of which is emitted within the building envelope. It is therefore important to be able to reliably predict electrical appliance use, in particular the magnitude and temporal variation of the energy use and power demand profiles arising from the aggregation of individual appliances, to support design and regulation of LV networks serving communities of buildings and of building's thermal systems.

But this is a complicated task, for the ownership and use of different types of appliance significantly varies from house to house, and between users. Addressing this diversity requires that we have an appropriate basis for allocating appliances to households depending on their composition and socio-economic characteristics and for predicting their subsequent use. This in turn implies the use of stochastic simulation and bottom-up approaches that may also facilitate the future testing of Demand Side Management (DSM) strategies.

So far, bottom-up approaches have focused on the modelling of high-load appliances: those that are commonly owned and which contribute significantly to total annual electricity use. Examples include cold (fridge and freezer), wet (washing machine and dishwasher) and cooking appliances. For example, the model of Jaboob et al.[2] predicts when the appliances are switched on, the duration for which they will remain on and their fluctuating power demands whilst on. But in our everyday lives we also use myriad low-load appliances. Their individual share of energy use may be small, in some cases even negligible, but it is significant when considering them as a group (or groups).

The objective of this paper is to find a parsimonious strategy for modelling four categories of low-load appliances: audio-visual, computing, kitchen and other appliances, which collectively account for those that are not represented by current device specific models. The work presented here extends and further develops that introduced in [3].

The remainder of the paper is organised as follows: section 2 introduces former work in the field; in section 3 the mathematical methods employed in the modelling are described, with their application presented in section 4, together with simulation results and evaluations of performance; section 5 concludes the paper.

2. Background

Bottom-up approaches describe the dynamics of a system by explicitly modelling the behaviour of the individual parts of that system. For the case of energy use, they consider the individual modelling of every end-use, or aggregates of them, in order to obtain aggregate profiles. These approaches are particularly promising given their potential for a) improving predictions of energy use of individual buildings or neighbourhoods when integrated with building energy simulation, b) sizing decentralised generation and storage devices, and c) testing Demand Side Management (DSM) strategies and rules for load management. Moreover, bottom-up approaches have the potential to explicitly include the effects of household composition and individuals' behavioural diversity.

Regarding appliance modelling, bottom-up approaches can be configured at different aggregation levels: from a pure microsimulation where each device is explicitly modelled, to strategies that consider aggregations of device for typologies of them.

Detailed microsimulation approaches are considered in probabilistic empirical models (as defined in [4]), which tend to model appliances one-by-one. Collected data, information on dwelling and household (occupants) characteristics, technical properties of appliances and aggregated values of energy use are combined in such approaches, and probabilistic methods are applied to generate results with profile diversity. Stokes' model [5] generates profiles at three aggregation levels: 30-minute-resolution average household, 30-minute-resolution specific household (with occupancy considerations) and 1-minute resolution specific household (including information relating to appliances' cycles). It considers 14 appliances plus miscellaneous, although only 9 different input monitored power cycles are taken into account, resulting in a limitation on the diversity of profiles generated, which in turn leads to poor results estimating the energy demand in the validation of the models. Paatero and Lund [6] introduce a social random factor (supposed to capture the social variety of the demand) that improves the diversity of patterns obtained; however, only yearly consumption data for the 16 end-uses is used for the generation of the models, together with other aggregate statistics, restricting the resolution to hourly time steps. In general, these approaches do not describe in terms of model parameters the dynamic behaviour of appliances, but they generate empirical profiles of power demand as a function of time.

Relatively more aggregated methods are models based on time-use-survey (TUS) datasets. In TUS datasets, the respondents fill in diaries of their activities during the day usually for one week periods, such as cooking, sleeping, travelling to work, etc. This data provides a powerful input to bottom-up models, since it encapsulates highly detailed information describing occupants' activities, that can be related to the use of appliances. To this end, Capasso [7] presents a first strategy linking occupants' activities with appliance use, using TUS data. The model produces 15-minute profiles of electricity use, considering aggregations of appliance that correspond to just four type of activities: cooking, housework, leisure and hygiene; each associated with a blend of large and small appliances, which are allocated by considering the average range of appliances present in the simulated household. The relation between performing an activity and using an appliance is described with a single coefficient *alpha* (defined as a human resources). Tanimoto [8] combines TUS with statistical data of ownership of appliances and its peak and stand-by powers. 31 activities are considered in this case, so that the level of aggregation is low, but this is contrasted by a small dataset size (58 households over 2 days).

In a similar vein, Widén [9] uses Swedish TUS data to model electricity use by assigning appliances to related activities (9 different categories in this case) and imposing five standard end-use profiles based on the type of their demand profile: demand disconnected from activity, power demand constant during activity, power demand constant after activity (with and without addition of temporal constraint) and fluctuating power demand (only applied to lighting). This approach is further developed in [10], where inhomogeneous Markov chains generate sequences of domestic activities that have an impact on power demand (5 minute and

1 hour granularity), including dependencies with the number of occupants performing these activities. A yet finer temporal resolution of 1 minute is achieved in the work developed by Richardson et al.[11]. Based on 7 different activities, a load curve for the appliances is created using the probability of switching on an appliance when an activity is being performed, and applying a fixed power conversion scheme. Using a calibration procedure based on the total time of use of an appliance, they obtain annual energy predictions. Although this tuning ensures a good overall match in annual energy demand, this does not imply the absence of compensating errors in the modelling of different appliance typologies, or that the dynamic characteristics of appliance use are well represented.

Although activity modelling is a promising method to obtain accurate energy demand profiles, this activity-appliance pairing approach does not facilitate the modelling of the range of appliances, because the activities that are recorded in time use surveys is insufficiently detailed, limiting the applicability of this approach to the modelling of either relatively high-load appliances or aggregations of small and large appliances for which there is weak empirical evidence. There has been no rigorous validation of those bottom-up modelling strategies to date, whether these are based on TUS data or not, to demonstrate their ability to faithfully capture energy use/power demand dynamics. These methods also have no rigorous basis for modelling the dependency of appliance ownership and related use characteristics as a function of household socio-demographic composition.

In partial response to these shortcomings, Jaboob [2] assigns (exclusively large) appliances to households as a function of their socio-demographic characteristics. The activities of the members of these households are then predicted, from which the conditional likelihood that related appliances will be switch on is modelled, as is the corresponding duration that they will remain on and their time-varying mean power demands whilst on. Thus, this modelling chain rigorously resolves for dynamic variations in mean power demand, in contrast to static power conversion schemes. Moreover, it presents the possibility of being used together with explicit models of low-load appliances, in order to obtain accurate values of the total electricity use of a house.

To this end and informed by these past endeavours, our task is develop a parsimonious strategy for the use of relatively low-load appliances, in complement to Jaboob's model of high-load appliances.

3. Methods

In this work we are interested in modelling the energy and power demands of low-load appliances to support building, systems and network design. In order to contribute to accurate predictions of residential energy use, we need to address the diversity in dwelling characteristics and human behaviours. Thus, we identify the following modelling tasks:

I Perform low-load appliance allocation, using cumulative distribution functions describing the peak power demand of aggregates of appliances. Devices are categorised into four groups: audio-visual, computing, small kitchen and other (miscellaneous housework, garden and personal care appliances).

II Model the characteristic use of these appliances in individual households. To this end, we utilise the fractional energy use f: the ratio of the actual to the maximum energy E_{max} that an appliance can use, determined by its rated power. Modelling f, we can distinguish between:

- Switching on/off events.
- Fluctuating demands whilst the appliances are in use.

Two considerations need to be taken into account in carrying out these tasks. Firstly, stochastic methods are required, as we are interested in describing the underlying randomness in households' appliance use and investment decisions. These methods rely on the definition of coefficients that represent the system as a probability distribution, which can be dependent on different variables such as time of the day, number of occupants, weather, etc. Secondly, using the normalized fractional energy f instead of absolute energy allows us to evaluate load profiles from different appliances of a similar type, but that do not necessarily have the same magnitude. In this way, appliances can be classified into groups and modelled as a category.

Candidate techniques that have been used to good effect in the modelling of occupants' behaviours include Bernoulli processes (activities [2]), discrete-time random or Markov processes (presence [12], blinds [13], windows [14]) and continuous-time random processes (blinds [13], windows [14]): the latter being a hybrid between discrete and continuous time random process models.

Furthermore, It has been previously shown [2, 9, 11] that stochastic methods are successful in describing energy demands and the information listed in Task II. In the work here presented, two of these statistical approaches have been exploited:

- *Discrete-time Markov processes* can model the probability of transitions occurring between energy states $s_i(t)$, with or without time dependency. Energy states are the result of discretising the range of fractional energy values. This discretization process can be more efficiently achieved if complemented with clustering techniques.

- *Survival analysis* can model the switching-on/off of appliances, as well as the duration an appliance remains in different energy states.

In the methodology presented here we have tested a range of strategies in order to find the most parsimonious approach. In this, we have ensured that the number of subjective decisions needed for modelling have been minimised, so that the methodology can be appropriately applied independently of the data set employed to estimate the models' coefficients.

3.1. Modelling fractional energy

3.1.1. Discrete-time Markov processes

A Markov process is a stochastic process that fulfils the Markov property, by which a future state depends on the most recent state, and not on any prior history [15]. A stochastic process $X(t)$ is therefore a Markov process if for every n and $t_1 < t_2 < \cdots < t_n$:

$$P[X(t_n) = x_n | X(t_{n-1}) = x_{n-1}, \ldots, X(t_1) = x_1] = P[X(t_n) = x_n | X(t_{n-1}) = x_{n-1}]. \quad (1)$$

Markov chains describe the process of making transitions between a present state i to a future state j, according to a probability distribution, described by a state transition probability matrix (or Markov matrix) as follows:

$$P_{ij} = \begin{pmatrix} p_{11}(t) & p_{12}(t) & \dots & p_{1m}(t) \\ p_{21}(t) & p_{22}(t) & \dots & p_{2m}(t) \\ \vdots & \vdots & \ddots & \vdots \\ p_{m1}(t) & p_{m2}(t) & \dots & p_{mm}(t) \end{pmatrix}, \tag{2}$$

where

$$p_{ij}(t) = \frac{n_{ij}(t)}{n_i(t)} = \frac{n_{ij}(t)}{\sum_j n_{ij}(t)} \tag{3}$$

is the probability that a transition from i to j takes place, given by the ratio of transitions that occur to state j from i to the total number of transitions occurring from i.

The dimensions of a Markov matrix $m \times m$ are given by the number of states m defined in the system. At the same time, the coefficients in the matrix may or may not depend on time. In the first instance, a time-homogeneous Markov process is considered, where the system can be described using a single matrix. We then consider a time-inhomogeneous Markov chain, in which the number of matrices r is given by the number of time slots considered to have different transition probabilities. For instance, if it is assumed that the probabilities are different for each hour of a day, then $r = 24$ (considering a single-day). This means that the probability distribution is given by a matrix of dimension $r \times m \times m$.

Appropriate dimensioning of the Markov matrices is not a trivial task: if m and r are set too low or even equal to 1, the dynamics or temporal variation of the system may not be suitably described by the model. On the other hand, if m and r are set too high, there is a risk of performing redundant calculations, adding unnecessary computing complexity, as well as a risk of overfitting the model.

In our case, fractional energy f is a continuous variable with values between 0 and 1, that is discretized into m energy states s. The time variable t is discrete, and it takes values every 10 minutes, but it can also be divided into r temporal states. In this sense, the subdivision chosen of the two-dimensional space $\{t, f\}$ generated by the time of the day and the fractional energy of a category of appliances will set the values of m and r, that determine the dimension of the transition matrix. Consequently, estimating an adequate and efficient subdivision of $\{t, f\}$ is key in the formulation of a parsimonious model. In our search for an objective methodology, clustering techniques were identified as good candidates to evaluate the partitioning of this space.

3.1.2. Matrix dimensioning: Density based clustering

Cluster analysis techniques provide a powerful and systematic mechanism for identifying groups or common features of a database D of n objects. There are a large number of clustering algorithms, two of the main being hierarchical and partitional [16] algorithms. The former decomposes D into a nested hierarchy of clusters, represented by a dendrogram, i.e. a tree diagram that splits the database into subsets of smaller size, until each object belongs to one subset. The process can be agglomerative or divisive, depending on whether the structure is made from the leaves towards the root or from the root to the leaves. The latter creates a single-level partition of D into k clusters based on similarity and distance measures. The parameter k is required as an input, even though it is not generally known *a priori*.

A third type of clustering method is density-based clustering algorithms, which apply local cluster criteria [17] in order to classify D. They identify regions of high density that are separated from other clusters by regions of a low density of points, which can be classified as noise. Each object of the database is evaluated in terms of density in the neighbourhood, which has to exceed some threshold. Density-based clustering algorithms present some advantages over other types of clustering:

(i) They are suitable for large data sets.

(ii) Clusters may have irregular shapes.

(iii) Although distance metrics are employed, clusters are identified based on density estimations of areas of the data set. The advantage of this is the identification of points that do not belong to any cluster, allowing for the treatment of unstructured (noise) points.

DBSCAN is a typical density-based clustering algorithm that was developed in 1996 [18]. The core idea behind DBSCAN is that for each object in a cluster, the neighbourhood of radius ϵ has to be populated with a minimum number of points *MinPts*. ϵ and *MinPts* are the two only parameters required.

However, the cluster structure of a real data set cannot usually be identified with a single global density parameter, but rather by clusters of different density, as well as their intrinsic structure. The OPTICS algorithm [17] is a generalization of DBSCAN. Instead of a clustering division, OPTICS outputs an ordering of the database relative to its density-based clustering structure, containing information for every density level up to a "generating distance" ϵ_0, that allows for analysis of the grouping structure (hierarchy). A graphical interpretation of the ordering is available through a reachability plot [17], where clusters are identified as "dents" in the plot. The authors of this algorithm provide a method for automatically determining the cluster hierarchy using the information extracted from the reachability plot. However, a simpler alternative method for automatic extraction of the clusters is described in [19], in which the most significant clusters are simultaneously selected from different density levels. Interestingly the authors also show that reachability plots are equivalent to the dendrograms of single-link clustering methods.

3.1.3. Survival analysis

Survival analysis [20] models the waiting time until a given event occurs, also referred to as *survival time*. Let T be a non-negative continuous random variable representing the survival time until an on-appliance is switched off (or an off-appliance is switched on); with probability density function (p.d.f.) $f(t)$ given by a Weibull distribution:

$$f(t) = \begin{cases} \frac{k}{\lambda}\left(\frac{t-\gamma}{\lambda}\right)^{k-1} e^{\left(-\frac{t-\gamma}{\lambda}\right)^k} & t > \gamma \\ 0 & t < \gamma \end{cases} \tag{4}$$

where $k > 0$, $\lambda > 0$ and $\gamma > 0$ are the shape, scale and location parameters of the Weibull distribution [20]. Thus, the cumulative distribution function (c.d.f.) $F(t) = P\{T < t\}$ gives the probability of the event to have occurred by duration t. The *survival function* $S(t) = 1 - F(t) = P\{T \geq t\}$ is then defined as the complement of the c.d.f, and describes the probability to remain in a given state before t:

$$S(t) = e^{-\left(\frac{t-\gamma}{\lambda}\right)^k}. \tag{5}$$

By inverting equation (5), it is possible to obtain directly the duration for which an appliance will continue (survive) in a specific energy state s as:

$$t_s = \gamma + \lambda \left[-\ln(w) \right]^{1/k}, \tag{6}$$

given a number $w \in [0, 1)$ drawn randomly from a uniform distribution.

Two cases have been studied in this work, either defining:

- Two energy states, s_0 for $f = 0$ and s_1 for $f \in (0, 1]$, corresponding to *on/off* states. Thus, switching on/off events are explicitly modelled.
- Eleven energy states, following an arbitrary division of 10 equidistant fractional energy states, plus the *off* state: s_i for $f = \{0;\ 0\text{-}0.1;\ 0.1\text{-}0.2;\ \ldots;\ 0.9\text{-}1\}$, respectively. Such a division of f allows us to test the added value of refined characterisation of energy states.

Therefore, occurrences of each event and durations are first extracted from the data, and used to fit Weibull distributions, obtaining scale, shape and location parameters λ and k. These distributions are then used to calculate survival times in a simulation using equation (6).

3.1.4. Monte Carlo simulation

Monte Carlo methods may be defined as *the representation of a mathematical system by a sampling procedure which satisfies the same probability laws* [15]. They provide a method to artificially represent a stochastic process by a sampling procedure, which will be determined by the particular underlying probability distribution of the given process.

For the specific problem posed here, the probability structure is given by either the parameters of the Markov chain or the survival analysis. In the former, a sequence of energy states $\mathbf{s} = \{s_0, s_1, \ldots, s_n\}$ is simulated, employing an inverse function method. For time t a random number is drawn from a continuous uniform distribution over the interval $[0, 1)$ and the corresponding interval in the c.d.f. is selected as the state for time step $t + 1$. This process is repeated for each time step in the simulation.

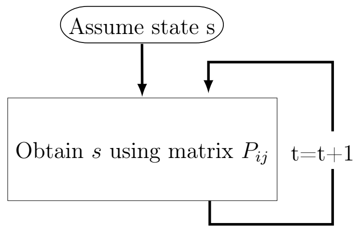

(a) Markov models.

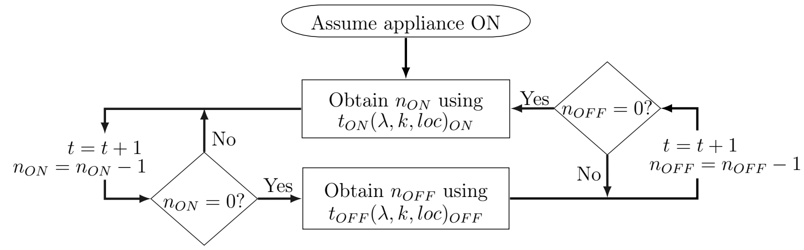

(b) *On/off* survival model.

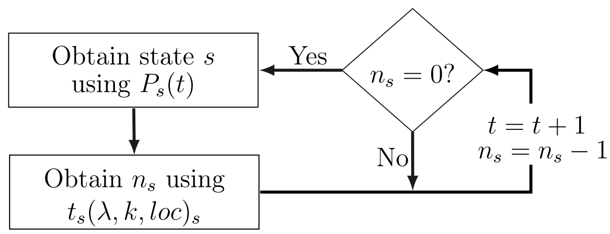

(c) Multistate survival model.

Figure 1: Simulation flowcharts.

For the latter case, equation (6) is employed -for an extracted random number w- to obtain the survival time t_s until a change of state occurs, covering a number n_s time steps. Temporal probabilities $P_s(t)$, extracted as the hourly likelihood of finding each of the states, are used to simulate the following state (this step is unnecessary for the *on/off* model, as there are only two states available: s_{ON} and s_{OFF}.). Thus, times and transitions between states are successively calculated for the simulation period, as outlined in figure 1. The key advantage of this approach is that it does not require calculations for the n_s time steps while the devices remain in the same state.

From energy states to an energy profile. The sequence of energy states $\boldsymbol{s}$ now needs to be transformed back into a fractional energy profile $\boldsymbol{f}_{sim}$. Thus, each energy-temporal state is multiplied by its corresponding mean or median fractional energy $\tilde{F}$, depending on the strategy employed, leading to a simulated fractional energy profile

$$\boldsymbol{f}_{sim} = \mathbf{s} \cdot \tilde{F}(\mathbf{s}). \tag{7}$$

One finale step transforms these profiles from fractional to actual energy values:

$$\boldsymbol{E}_{sim} = \boldsymbol{f}_{sim} \cdot \tilde{E}_{max}, \tag{8}$$

where $\tilde{E}_{max}$ is a statistical measure of the maximum energy (or power $\tilde{P}$ as required) for all instances in the category. Thus, the estimation of $\tilde{E}_{max}$ values becomes critical to calculating accurate aggregate energy profiles. Assignment of the maximum energy can be performed using c.d.f.'s of the relevant appliance categories, or else using simple mean or median measures.

Although assignment of $\tilde{E}_{max}$ is important, it is also trivially complicated. In what follows then, we focus on testing the underlying hypothesis in our modelling strategies rather than in the fidelity of predictions of aggregate energy profiles that require a random assignment process.

3.2. Household Electricity Survey data set

The Household Electricity Survey [21] is an extensive monitoring survey of 250 households in the UK, carried out during 2010 and 2011. Apart from detailed socio-demographic information, it contains data describing the appliances present in every monitored household and their temporal electrical energy use during 1 or 2 months, with records every 2 minutes. Of the 250 households, 26 of them were additionally monitored for a whole year, with 10 minutes resolution. Since the one-month data was not measured during the same month for all households, only the data recorded for the 26 houses during a whole year was utilised in the analysis presented here, in order to avoid possible seasonal effects on the use of appliances.

The relevant low-load appliances found in the dataset were classified into four categories, following the type of activity that involves their use:

- audio-visual (excluding TVs, that are considered as high-load appliances given their extensive use),

- computing,

- small kitchen appliances (excluding cookers, microwaves and ovens),

- other small appliances.

Figure 2 shows the types of device available in the data set and their contribution to annual energy use, with categories depicted in different colours. The height of the bars represents the mean value of annual energy use of the corresponding type of appliance, whereas the width is proportional to the number of instances observed in the 26 households for the given device. Thus, the area of the bar indicates the total energy use of that appliance throughout the stock of houses surveyed.

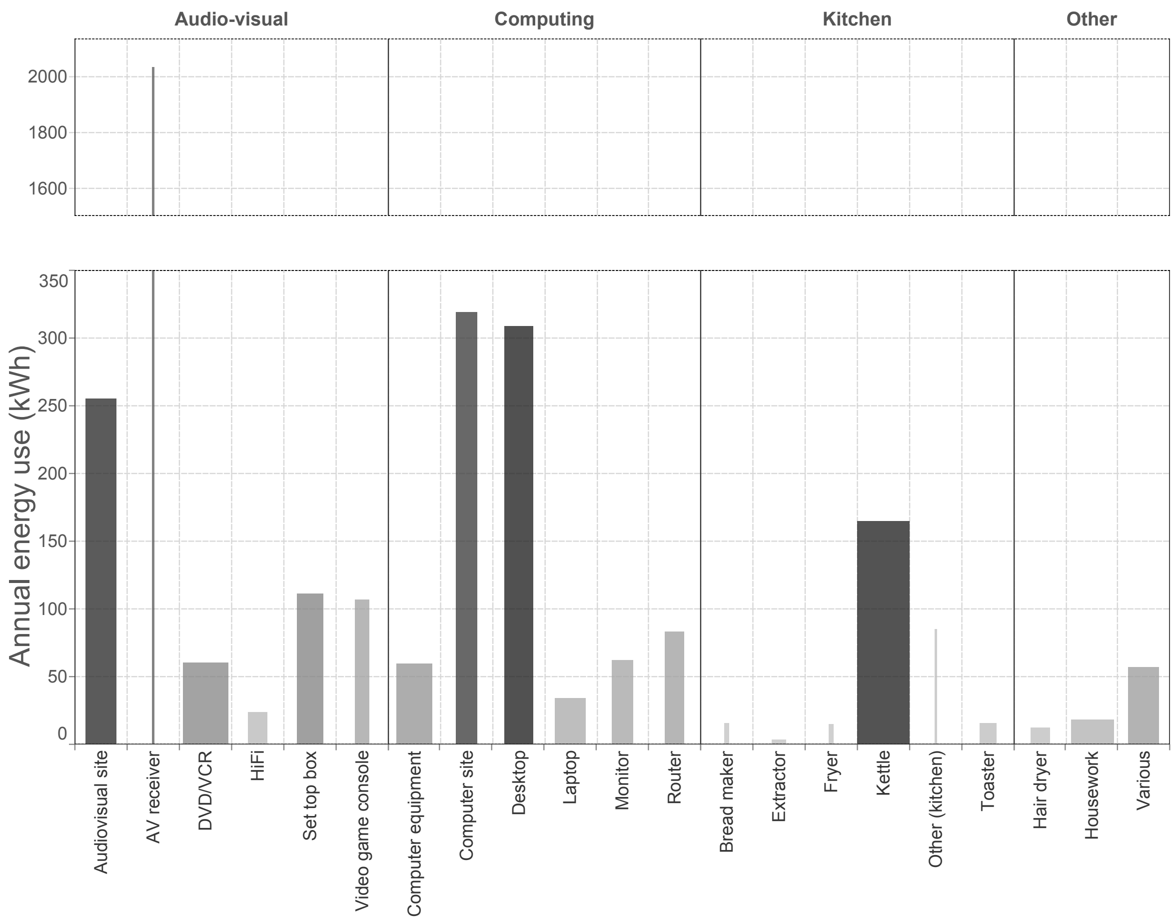

Figure 2: Annual energy use of the types of appliances considered in the modelling, divided in four categories: audio-visual, computing, kitchen and other. The height of the bars corresponds to the mean annual energy use, while the width is proportional to the number of instances recorded in the 26 houses. Combining this information, darker bars identify the dominant types of appliance for the category.

One shortfall encountered in the data set is that there is no information describing the rated power of the appliances, posing a challenge to the accurate estimation of E_{max}. Consequences derived from this and the solution proposed are discussed in section 3.2.2.

The procedure adopted in our work was to test a range of strategies to model one appliance category, the audio-visual category, in order to identify the most parsimonious approach, and then to deploy this to other categories of appliance.

3.2.1. Audio-visual category

In this section the nature of the data used to test the modelling techniques is presented. Table 1 displays the total number of instances of each subcategory of appliance considered in the audio-visual category, present in the 26 houses, leading to a total of 102 instances for the category. Our first step was to extract fractional energy values from the electricity use records, as

$$f = \frac{E}{E_{max}}. \tag{9}$$

Type of appliance	**Number instances**	$\tilde{E}_{before}$ (Wh)	$\tilde{E}_{after}$ (Wh)
AV receiver	1	86.4	86.4
Audio-visual site	33	42.4	34.9
DVD/VCR	28	8.2	5.41
HiFi	14	33.1	29.4
Set top box	17	5.2	5.2
Video-game console	9	19.9	16.7

Table 1: Types of appliances available in the audio-visual category: number of instances (each device in each house) and mean maximum energy for the subcategory, before ($\tilde{E}_{before}$) and after ($\tilde{E}_{after}$) applying outlier filters (as explained in section 3.2.2).

Given an estimate of $\tilde{E}_{max}$ this transformation outputs a normalised profile for each appliance in each house with values in the interval $f \in [0, 1]$, that can be combined now with other instances or other types of device, allowing the category to be modelled. It is also possible to explore how these profiles vary during the period of a day, in order to identify patterns or dominant behaviours. Interesting characteristics of the data set include that:

i. The data set contains over 4.2 million data points.

ii. 33.9% of the data are zero values ($f = 0$), suggesting that appliances are off for around a third of the time.

iii. The off-state exhibits temporal dependency, reaching maximum values in the early hours of the morning (39%) when most people are sleeping, and a minimum (29%) between 20h and 22h, when most people are present and awake.

iv. 15% of the entries have fractional energy lower than 0.1, which likely corresponds to a stand-by state, a common feature of audio-visual devices.

v. As with iii., a concentration of stand-by states is found during the early hours of the day, whereas appliances are most often used at maximum power during the late hours of the evening.

A preliminary visualization of the two-dimensional space created by the time period of a day and the fractional energy values $\{t, f\}$, is depicted in figure 3. Dark areas represent denser regions of the data set, showing common values recorded during certain times of the day. Values of $f = 0$ were excluded to help with the interpretation.

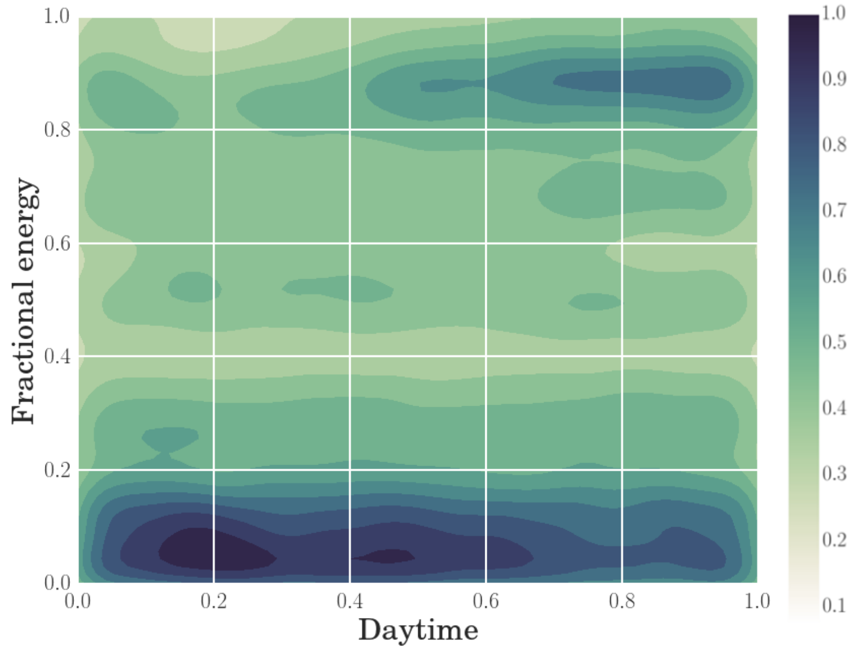

Figure 3: Distribution of audio-visual category data, for the values of fractional energy over a day (normalised values). A sample of 50000 entries is plotted. Since the data set contains a large amount of values with $f = 0$, these data were excluded to facilitate comparison between other values.

3.2.2. Data preprocessing: outliers and maximum energy estimation

As previously mentioned, our data set does not include appliance name plate (power) ratings. The fractional energy modelling approach, however, is dependent on the values of E_{max} and requires this input at two specific stages. Firstly in using equation (9) to extract fractional energy profiles for each instance. Secondly after the simulations have been performed, to compute an energy profile from a simulated fractional energy time-series for the category.

In order to estimate E_{max} from the data, the maximum energy record for each profile was used. The existence of discrepant entries for the same type of appliance suggested that a data cleaning process was necessary. This could be due to the fact that each data point represents the energy corresponding to the mean power drawn by an appliance over a period of ten minutes. Since this may fluctuate between 0 and the nameplate rating it could be that the calculated value of E_{max} results from an appliance that has been working at higher power during a shorter period of time (*e.g.* a kettle that never takes 10 minutes to boil). This problem was overcome by obtaining maximum energy values from the 2-minute data (also subjected to a cleaning pre-process), with the purpose of selecting consistent entries.

A Seasonal Hybrid Extreme Studentized Deviate test (S-H-ESD) [22] was employed to detect anomalies. S-H-ESD is based on the generalized ESD algorithm to detect one or more outliers in a univariate data set that follows an approximately normal distribution, and is applicable to time-series data. Its main feature is that it is able to predict both local and global anomalies, taking into account long-term trends on the temporal profile to minimize the number of false positives. In other words, the conditions to detect an outlier vary depending on local temporal windows. When no trend is identified, the algorithm works as an ordinary outlier filter. The algorithm is part of the *AnomalyDetection* package in R [23].

The result of applying the outlier filter is presented in table 1 as the mean maximum energy per subcategory of appliances in the audio-visual data set before and after the outlier test. For some categories the exclusion of outliers leads to a discrepancy on the estimation of E_{max} as large as 300%.

3.3. Validation methods

3.3.1. Cross validation

In statistical modelling, cross-validation processes are used to assess how effectively the results will generalize to a different data set [24]. Cross-validation computes the average error obtained from evaluation measures of different partitions of the data set. There are several methods for cross-validation, such as random sub-sampling, leave-one-out cross validation and K-fold cross validation. In our work we favour K-fold cross validation in which the data set is partitioned in to K subsamples. A single subsample is used as the validation set and the remaining (K-1) subsamples are used as the training set. This process is then iteratively repeated K times (*folds*), until each partition has been used once as a validation set. A mean performance error can then be computed as the average error:

$$e = \frac{1}{K}\sum_{i=1}^{K} e_i, \tag{10}$$

where e_i represents some error between prediction $\hat{y}_i$ and observation y_i. K-fold cross validation is a computationally expensive method, but produces an accurate estimation of the goodness of fit.

3.3.2. Time series analysis

Selecting an adequate strategy for the modelling of fractional energy requires a comparison of performance between simulation and observation data sets during the validation period. Time series analysis provides a powerful method to compare and understand internal structure on both temporal profiles, extracting meaningful statistical information. The objective is to describe the validation time series with a set of parameters that should be replicated by the simulation time series. In particular, it is possible to decompose the fractional energy profile into trend, seasonal and irregular (or remainder) component, allowing for evaluations of each of the components at a different level. Figure 4 shows an example of a decomposed time series.

The following information is used from the decomposition exercise:

- *Trend component.* The observed data presents a flat trend curve. Therefore, the mean value of the trend component of both simulation and observation can be used for comparison, giving an idea of the average fractional energy expected.

- *Seasonal component.* A daily period (or seasonal component) is expected in the use of appliances. The models are expected to reproduce this periodicity correctly, and this can be studied using the cross-correlation function [25] between two signals (X_t, Y_t), which is defined as

$$\rho_{XY}(\tau) = \frac{1}{N-1}\frac{\sum_{t=1}^{N}\left(X_t - \mu_X\right)\left(Y_{t+\tau} - \mu_Y\right)}{\sigma_X\sigma_Y}, \tag{11}$$

  where μ_k, σ_k are the mean and standard deviation of process $k = X, Y$, respectively, and τ is the lag or time delay between both. Equation 11 provides an insight into the relationship and dependence between observed and simulated periodic components. Based on that, we examine:

  - Pearson's coefficient, as an index of the linear correlation at $\tau = 0$ (considering both signals to be synchronised); ideally this should be equal to 1.
  - Time delay of maximum correlation, in order to determine whether the signals are in phase with each other.

- *Irregular component.* After extracting the trend and seasonal components, a residual fluctuating variation remains.

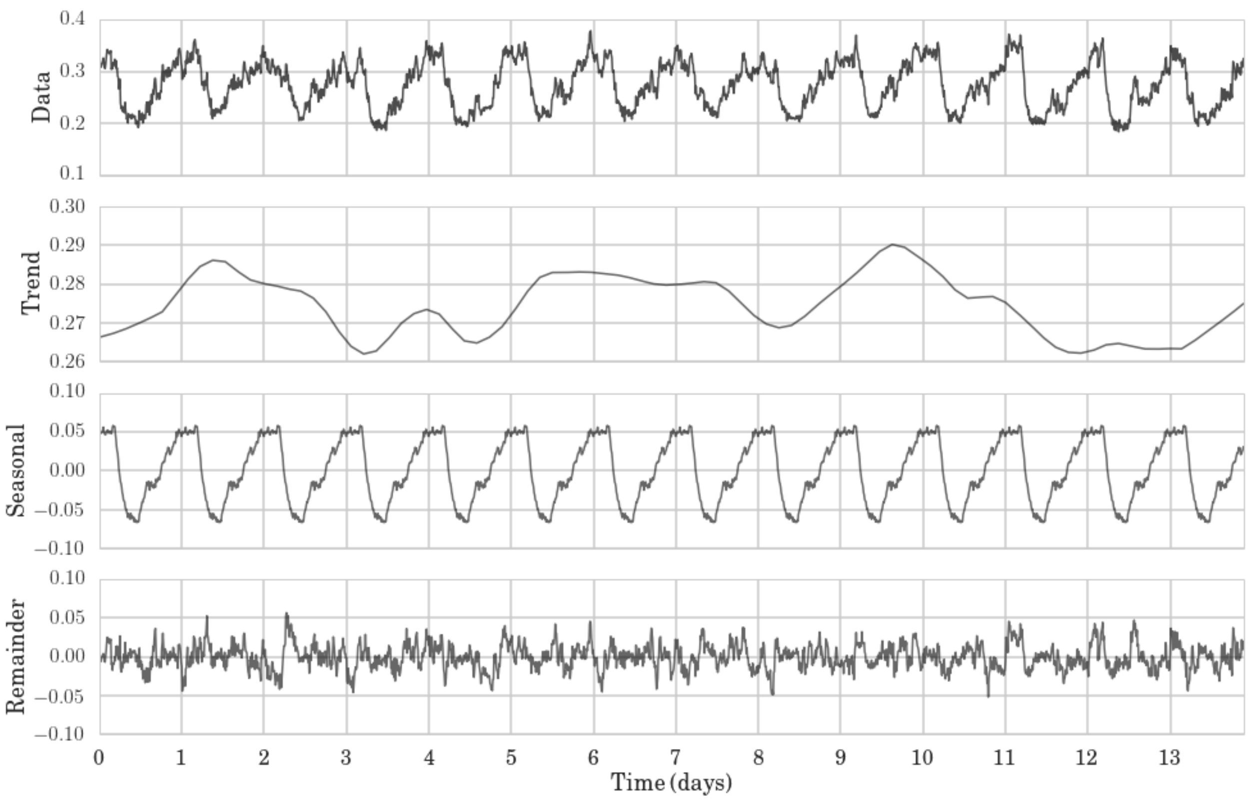

Figure 4: Example of time series decomposition into trend, seasonal and remainder component.

3.3.3. Sensitivity and specificity analysis

Sensitivity and specificity analysis represents a strong indicator of the model's absolute aggregate performance: its ability to correctly reproduce the time dependent properties of the process being simulated. Sensitivity or true positive rate (TPR) is defined as the proportion of matching cases between simulated and observed values, i.e.:

$$TPR = \frac{TP}{TP + FN}, \tag{12}$$

where T, F, P, N represent True, False, Positive and Negative and TP is the total number of truly predicted positive outcomes (true positives). Specificity or true negative rate (TNR) is defined as [26]:

$$TNR = \frac{TN}{TN + FP}. \tag{13}$$

In an ideal case, one would have $TPR = 1$ and $TNR = 1$ (or $FPR = 1 - TNR = 0$). Comparison of these indicators can be plotted in receiver-operating characteristic (ROC) space. This analysis can be complemented with the model accuracy

$$ACC = \frac{TP + TN}{P + N}, \tag{14}$$

giving an indication on the overall performance of the model. For multi-state systems (as in our case, with multiple energy states) this is a particularly exigent evaluation technique.

3.3.4. Application of validation methods

In this work, 10-fold cross validation is performed for every approach suggested. For each iteration, several error measures at three different levels have been taken into account:

1. At the first level, we are interested in evaluating the quality of the fractional energy signal produced by our simulations. *Time series decomposition* has been performed (section 3.3.2) to extract the following comparative measures:

    - Relative error of the expected value of the trend component.
    - Pearson's coefficient and time delay of maximum correlation of the seasonal component.

2. We are also interested in evaluating the accuracy of the averaged daily profile of fractional energy, as well as the models' effectiveness in predicting energy states. For this we use:

- *Simulated energy states.* Sensitivity and specificity analysis is directly applied to the simulated energy states, producing ACC values and an ROC plot.
- *Absolute state prediction.* The probability of predicting each of the states during the validation period is calculated and compared for observation and simulation. Discrepancies between both magnitudes are represented with RMSE.
- *Temporal probability of state prediction.* The probability distribution for each state over time provides insight into the temporal variation of each state, allowing us to identify situations when some states are over or under-predicted, and even at which periods during the day. Discrepancies again are calculated with RMSE.
- *Fractional energy daytime profile.* Once the energy states have been converted into fractional energy values, it is possible to evaluate the results for a typical day over the validation period (averaged over all the days for which fractional energy values are available for each time step). Residuals and RMSE are calculated to describe performance.

3. Finally, the selected methodology should perform well in calculating *total energy use.* Each simulated instance is converted to an energy profile using maximum energy values of the appliances present. The total energy use over the validation period is then obtained and compared for the relevant category of appliance.

The validation data set is a subset of the data that corresponds to 10% of the available total time range. This subset does not contain a unique time series of values, but a number q equal to the number of instances in the category. The simulation of energy states was performed q times over the validation period, in order to perform the sensitivity and specificity analysis for the energy states. For the other evaluation measures, averaged values for all instances were considered for both observation and simulation.

4. Results and discussion

In this section we first explain the application of the techniques presented in 3.1.1 and 3.1.3, respectively, to the data set introduced in section 3.2. Then, simulation results are described and evaluated for each of the strategies tested to model fractional energy use of audio-visual appliances, justifying the selection of one of them. Finally, the selected strategy is applied to the other appliance categories, and a final evaluation of the model is given.

4.1. Application of Markov model

As a first approach, the $\{t, f\}$ space was arbitrarily divided with $m = 11$ (11 energy states: one for the off-state plus ten of 0.1 fractional energy width) and $r = 24$ (one temporal state per hour), leading to 264 subdivisions.

Clustering techniques were then applied to the audio-visual appliances data set. Excluding entries when the appliances are switched off (i.e. $f = 0.0$), there are over $2.8 \cdot 10^6$ data points (from a total of over $4 \cdot 10^6$), which is still large given the computational expense of the clustering algorithms used. In order to overcome this problem, a random sampling process [27] was carried out, selecting 50,000 points that roughly represent 2% of the total size of the data set.

Implementations of the DBSCAN and OPTICS algorithms were tested, corroborating that the unique global density parameter of DBSCAN was not effective at finding a satisfactory partition of the data set into clusters; since we are interested in finding clusters of different density.

Subdivision of $\{t, f\}$ *space.* The objective of applying a density-based clustering algorithm (OPTICS) is to produce an efficient subdivision of the two-dimensional space $\{t, f\}$, as described in section 3.1.1. As summarised graphically in 5, the process works as follows:

1. Find parameters that produce a good clustering structure.

2. Adjust the clusters found to fit a cell of rectangular shape. In order to avoid overlapping of cells, data points between the 1st and 99th percentile are selected for each cell. Points identified by OPTICS as noise are grouped into noise cells that will fill the empty space not covered by the clusters.

3. Define the grid established by the edges of the rectangles.

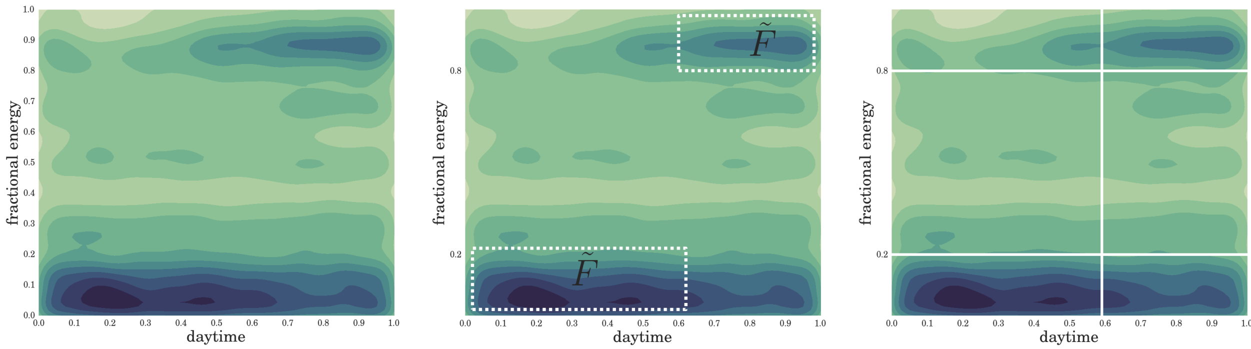

(a) Data (b) Cluster identification (c) 2×4 Markov matrix

Figure 5: From the data: (a) clusters are identified by the algorithm allowing rectangles ranging from the 1st to 99th percentiles to be extracted (b); the rest of the space will be divided into noise cells. From that, a grid is defined, (c) whose partitions will be the dimension of the matrix (taking into account the off state $f = 0$), associating with each cell the median value of fractional energy $\tilde{F}$ of the data points it contains.

4. Associate with each cell a fractional energy value $\tilde{F}$ corresponding to the median value of the points it contains.

OPTICS requires two parameters to produce the ordering of the points: first, the generating distance ϵ_0, referring to the largest distance considered for clustering (clusters will be able to be extracted for all ϵ_i such that $0 < \epsilon_i < \epsilon_0$); second, the minimum number of points that will define a cluster *MinPts*. However, the algorithm used to automatically extract the clusters from the ordering of the points and their reachability distance makes use of a further 7 parameters [19], upon which the clustering structure obtained will vary. For this work, the OPTICS algorithm was implemented in Python[1].

After a systematic search for a well performing solution, a set of successful parameters was identified[2]. These values lead to a hierarchical solution, with four incremental nested partitions, from two clusters at the top level of the hierarchy, to eleven at the leaves. The four

[1]Aided by script provided in `https://github.com/amyxzhang/OPTICS-Automatic-Clustering.git`

[2]Parameters found following description in [19] are: $\epsilon = 0.08$; $MinPts = 50$; $minClustSizeRatio = 0.03$; $minMaximaRatio = 0.001$; $significantMin = 0.003$; $checkRatio = 0.8$; $maximaRatio = 0.87$; $rejectionRatio = 0.8$ and $similarityThreshold = 0.6$.

different levels (summarized in Table 2) lead to four different divisions of the $\{t, f\}$ space and four Markov matrices with different dimensions. The relative performance of these different structures is evaluated in the following sections.

Name	**Hierarchy level**	**Clusters**	**Noise cells**	**$\{t, f\}$ dimension**
OPTICS - 5x15	IV	11	9	5x12
OPTICS - 4x14	III	10	5	4x12
OPTICS - 3x11	II	7	4	3x11
OPTICS - 1x3	I	2	None	1x3

Table 2: Hierarchical levels of clustering considered for $\{t, f\}$ space partition, with number of clusters and number of noise cells identified.

4.2. Application of Survival analysis

The two alternatives considered for the survival models are a simple two-state (on-off) model and a multistate model with 0.1 divisions in f, so that there are eleven states in total (*cf.* 3.1.3). This multistate model encapsulates temporal variations since the transitions to the following state are computed based on the temporal probability of finding each of the states. Weibull parameters (shape, scale and location) introduced in equation (4) are estimated from the data points for each of the energy states. Once obtained, the simulation runs as depicted in figure 1b.

4.3. Approach selection

The fractional energy use of the audio-visual category of appliances was modelled using a range of strategies. The goodness of fit of the models is evaluated from different points of view, following the description in section 3.3.4.

4.3.1. Fractional energy time series

Decomposition of the time series over the validation period allows for the extraction of statistical information from the structure of the observed and simulated data and to compare their different components: trend, seasonal and remainder (see section 3.3.2).

Trend. The trend component presents a constant value over the whole year of observed data, so there is no need to fit a function. It gives an estimation of the mean value of the fractional energy, given that the daily seasonality has been removed. The trend can be used to indicate a relative error from the simulations, as shown in table 3.

Seasonal component. The seasonal components are shown in figure 6, plotted for several days. There are two models, OPTICS-1x3 and Survival, for which an inadequate handling of dynamics is clearly apparent. For the other cases, those with larger numbers of temporal states produce an understandably more accurate seasonal profile (11x24-SHESD, OPTICS-5x14, with 24 and 5 temporal states, respectively). Also, the Survival Multistate model represents surprisingly well the daily seasonality, considering that the temporal dependency is included only in the transitions between states, but not in their duration.

Table 3 complements those results with numerical values for Pearson's coefficient and temporal lag at maximum correlation. Again, the best value for Pearson's coefficient and time lag is achieved using the models with a larger number of temporal states 11x24-SHESD and Survival Multistate, followed by OPTICS-4x12 and OPTICS-5x14.

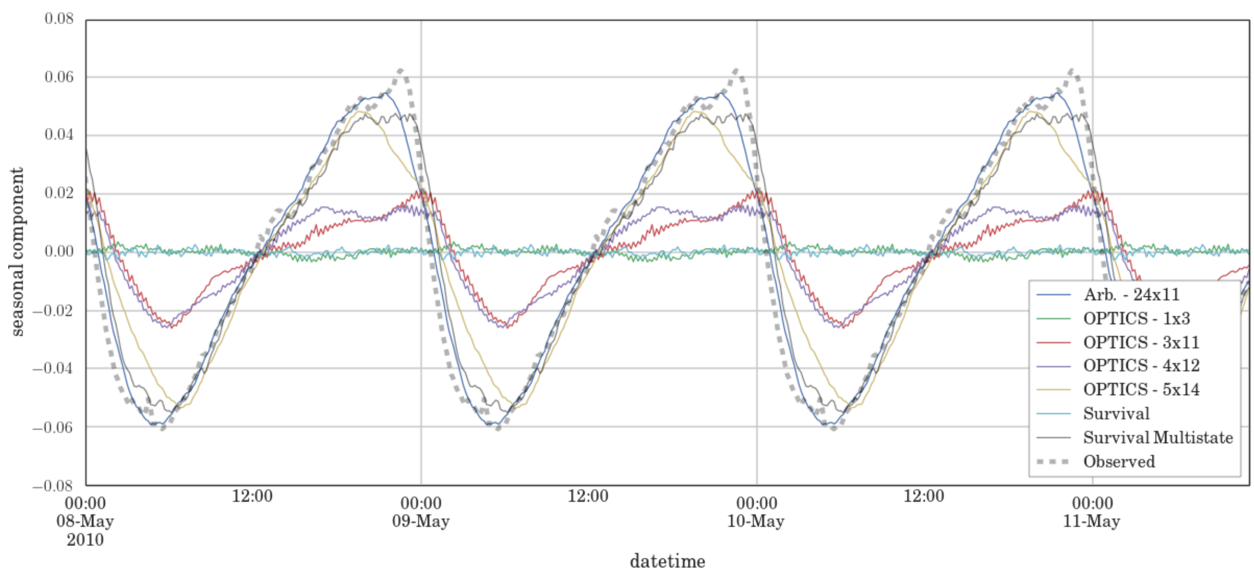

Figure 6: Comparison of seasonal components.

	Rel. error trend	Pearson's coeff.	lag
Arb - 24x11	2.35%	0.989	0.0
OPTICS - 5x14	5.08%	0.9501	−0.0278
OPTICS - 4x12	4.91%	0.960	−0.0486
OPTICS - 3x11	5.40%	0.854	−0.0625
OPTICS - 1x3	3.83%	−0.446	−0.424
Survival	0.831%	−0.0896	0.236
Survival multistate	5.61%	0.983	−0.0208

Table 3: Summary of validation time series decomposition. From left to right: error on the average value of the trend; Pearson's correlation coefficient and time delay (lag) of seasonal component. "Arb" refers to the arbitrary subdivision of the data into 24 time states and 11 fractional states.

4.3.2. Evaluation of average daily profile

In the previous section the signal simulated over the whole period was compared; but we are also concerned with how well the averaged daily profile is represented, in terms of the predictive power of simulated energy states and the consequent fractional energy profile.

Fractional energy states prediction. Figure 7 shows the dependency of the RMSE (calculated for every 10-minute timeslot) with time for the probability of finding the system in each of the defined energy states. The *on/off* Survival approach gives RMSE values an order of magnitude larger than for the Markov models, indicating a poor overall estimation of the two states considered. Since there are only two states defined, their probabilities of being simulated are complementary, $P_{s=0}(t) = 1 - P_{s=1}(t)$; therefore, a poor estimation of $P_{s=0}(t)$ implies a poor estimation of $P_{s=1}(t)$.

Furthermore, the shape of the curves for Survival and OPTICS-1x3 models implies that the temporal dependency of the system is not well encapsulated. The former exhibits an increase in error during the late hours, suggesting a worse prediction of the on-state; while the RMSE in the latter increases both in the evening and during the night, revealing an under performance for both the off state and the maximum energy state.

Temporal dependency is well represented in the Survival Multistate model, although the overall error in energy state prediction is slightly higher than with the Markov approaches. This could suggest that the specific energy states are better represented when clustered energy values have been considered.

The total RMSE for temporal and absolute (not temporal) daily state predictions are presented in table 5. In both cases, OPTICS-5x14 outperforms the other strategies, suggesting that the larger the number of energy states (14 in this case), the more accurate the probability prediction.

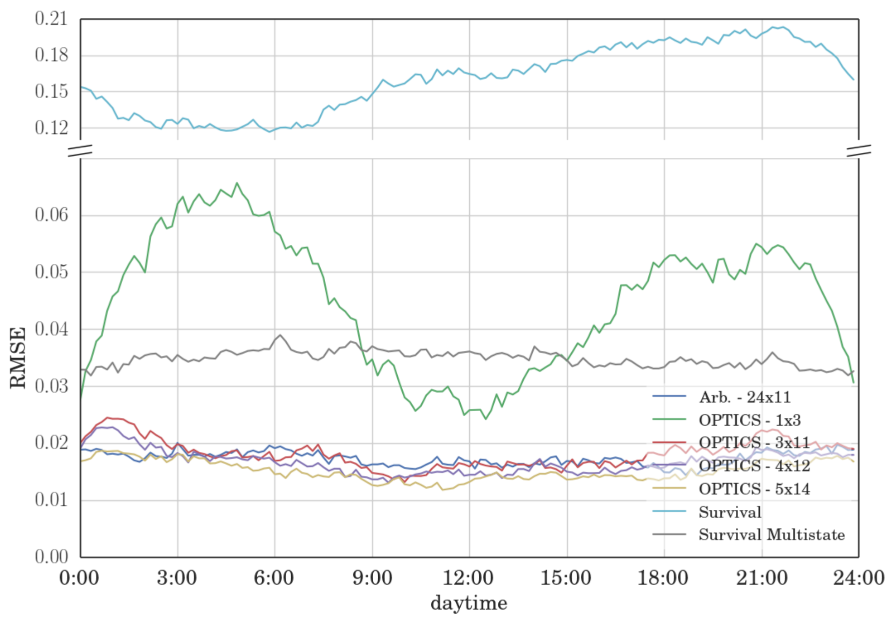

Figure 7: Temporal dependency of RMSE, calculated for each 10-minute time slot, for all states of each approach.

As noted in section 3.3 the accuracy of the modelling of states can also be evaluated using ROC parameters, as shown in table 4; although this is a particularly onerous test when applied to multi-state systems, so that TPR is not expected to be high. Once again the OPTICS 5x14 and Survival Multistate models outperform their counterparts.

Fractional energy averaged daily profile. The residuals in fractional energy for an average day tend to increase towards the boundaries of the day (Figure 8), where users are more active

	TPR	TNR	ACC
Arb - 24x11	0.173	0.917	0.483
OPTICS - 5x14	0.160	0.935	0.487
OPTICS - 4x12	0.172	0.925	0.485
OPTICS - 3x11	0.178	0.918	0.483
OPTICS - 1x3	0.339	0.669	0.456
Survival	0.499	0.499	0.450
Survival multistate	0.189	0.919	0.484

Table 4: Accuracy of model.

in switching devices and regulating them. Nevertheless, the results suggest that even with temporally crude models, dynamics are well encapsulated (with the exception of OPTICS-1x3 and Survival); particularly in the case of the model with the largest number of temporal states, Arb.-24x11, as reflected in table 5.

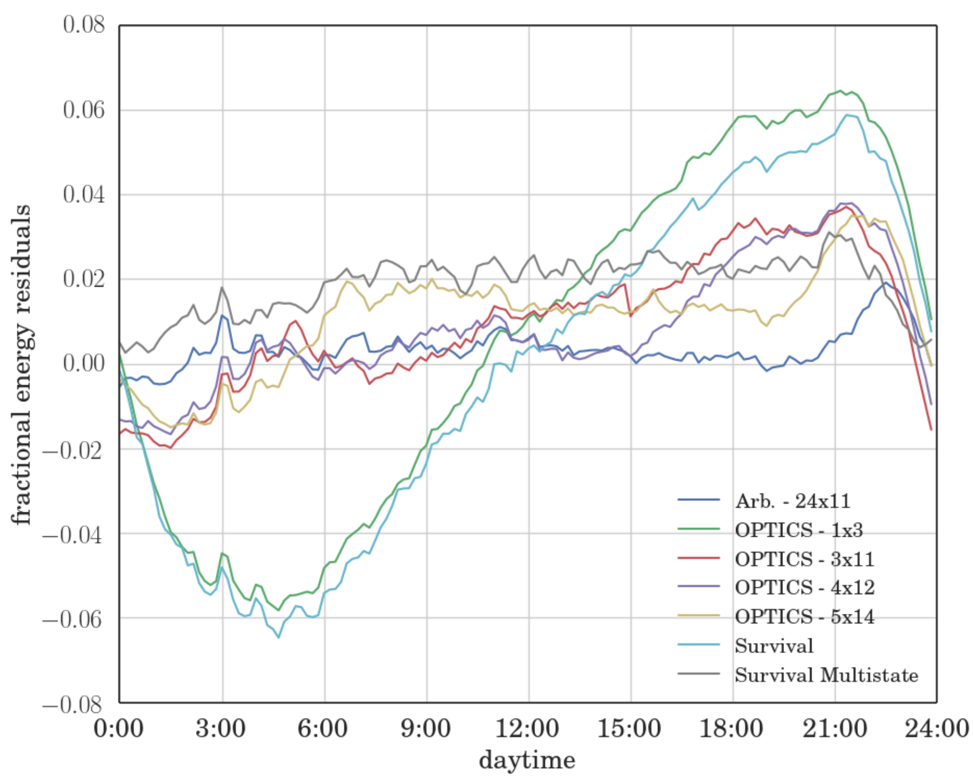

Figure 8: Daily profile residuals of fractional energy.

	Fractional energy (f)	Absolute state prediction	Temporal state prediction
Arb - 24x11	$2.056 \cdot 10^{-2}$	$2.00 \cdot 10^{-2}$	$1.76 \cdot 10^{-2}$
OPTICS - 5x14	$2.32 \cdot 10^{-2}$	$1.86 \cdot 10^{-2}$	$1.56 \cdot 10^{-2}$
OPTICS - 4x12	$2.54 \cdot 10^{-2}$	$2.06 \cdot 10^{-2}$	$1.73 \cdot 10^{-2}$
OPTICS - 3x11	$2.70 \cdot 10^{-2}$	$2.23 \cdot 10^{-2}$	$1.89 \cdot 10^{-2}$
OPTICS - 1x3	$4.66 \cdot 10^{-2}$	$1.84 \cdot 10^{-2}$	$4.85 \cdot 10^{-2}$
Survival	$4.22 \cdot 10^{-2}$	$1.13 \cdot 10^{-1}$	$1.63 \cdot 10^{-1}$
Survival multistate	$2.53 \cdot 10^{-2}$	$3.55 \cdot 10^{-2}$	$3.50 \cdot 10^{-2}$

Table 5: RMSE values of the daily profile results, in terms of the fractional energy profile, absolute state prediction (without temporal dependency), and temporal state prediction.

4.3.3. Total energy prediction

For the total energy prediction over the validation period, a random assignment process of maximum energy values is performed for each of the instances' fractional energy simulations, as explained in section 3.1.4.

In order to compare the results, a box plot is presented in figure 9, and the residual error in energy use prediction is presented in table 6. Whilst the median residual error is in all cases relatively low, the simulated values are consistently positively skewed, overestimating the upper quartile in total energy use. This is caused by a loss of information during the modelling process. Errors compound from the modelling of fractional states, through the assignment of maximum energy values to the subsequent prediction of energy use for the relevant appliance category. Thus, even though each task in our modelling process faithfully reproduces reality, errors inevitably arise when using models estimated from aggregate data of the four typologies of appliance to the prediction of specific device behaviours; errors that will reduce in magnitude as the size of the stock of appliances simulated increases. This is reasonable considering that our goal is to estimate communities of buildings and the appliances contained within them.

	Mean Residual (kWh)	Median Residual (kWh)
Arb - 24x11	−13.5	−1.83
OPTICS - 5x14	−13.5	−1.76
OPTICS - 4x12	−12.7	−1.43
OPTICS - 3x11	−12.5	−1.48
OPTICS - 1x3	−11.8	−1.68
Survival	+1.13	+1.80
Survival multistate	−11.6	−1.44

Table 6: Residual error between observation and simulation, for mean and median of the total energy use over the validation period.

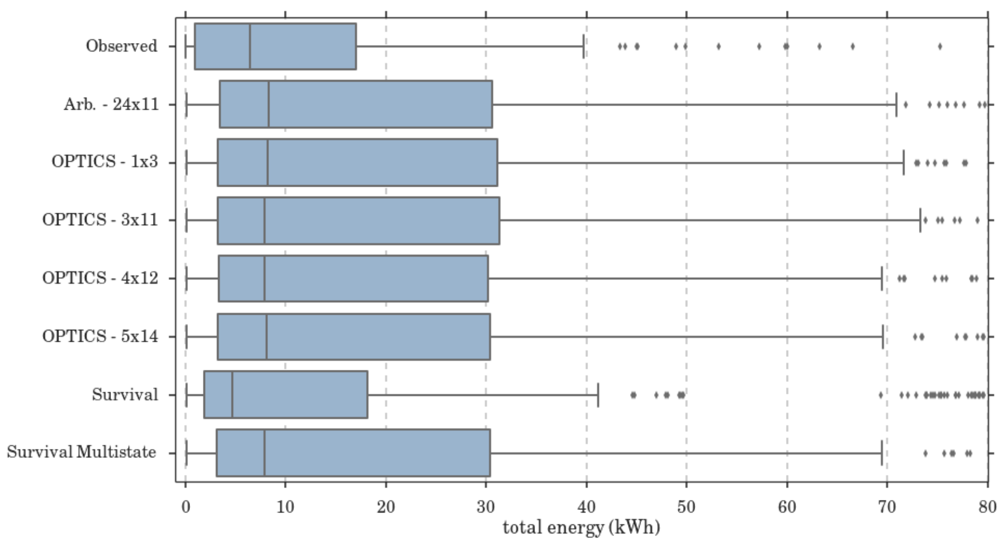

Figure 9: Boxplot comparing observed and predicted total energy use over the validation period.

4.3.4. Summary

The complexity of the different approaches can also be used for comparison, based on the type and number of parameters that the models need. They are summarised in table 7.

For the Markov based approaches, the parameters needed are those that build the Markov matrix, and are dependent on its dimension. Additionally, the clustering process requires 9 extra parameter values, which are not easily extracted, as the clustering algorithm requires a trial and error process which is complicated and time-consuming. The parameters needed in the survival models are those that describe the Weibull distribution, plus the hourly probability distribution of each state to occur (trivial to obtain and which can be simplified using less time slots.)

	Number of parameters	**Type**
Arb - 24x11	24×11	Markov matrix
OPTICS - 5x14	$5 \times 14 + 9$	Markov matrix and clustering
OPTICS - 4x12	$4 \times 12 + 9$	Markov matrix and clustering
OPTICS - 3x11	$3 \times 11 + 9$	Markov matrix and clustering
OPTICS - 1x3	$1 \times 3 + 9$	Markov matrix and clustering
Survival	3×2	Weibull parameters
Survival multistate	$3 \times 11 + 24 \times 11$	Weibull and states' probability

Table 7: Number and type of parameters needed for the different type of model.

To inform our selection of the most parsimonious modelling strategy the relative performance of each of the models tested is qualitatively summarised in figure 10, using a color coded diagram. From this it is apparent that the Survival Multistate strategy outperforms its counterparts: its predictive power is comparable to that of the more refined Markov models, but is considerably simpler in formulation, both in the estimation of its coefficients and in subsequent implementation. It performs well in the time series analysis, temporal state prediction and fractional energy profile, acceptably well in absolute state prediction, accuracy and total energy use. For these reasons, the Survival Multistate approach has been deployed to model the other categories.

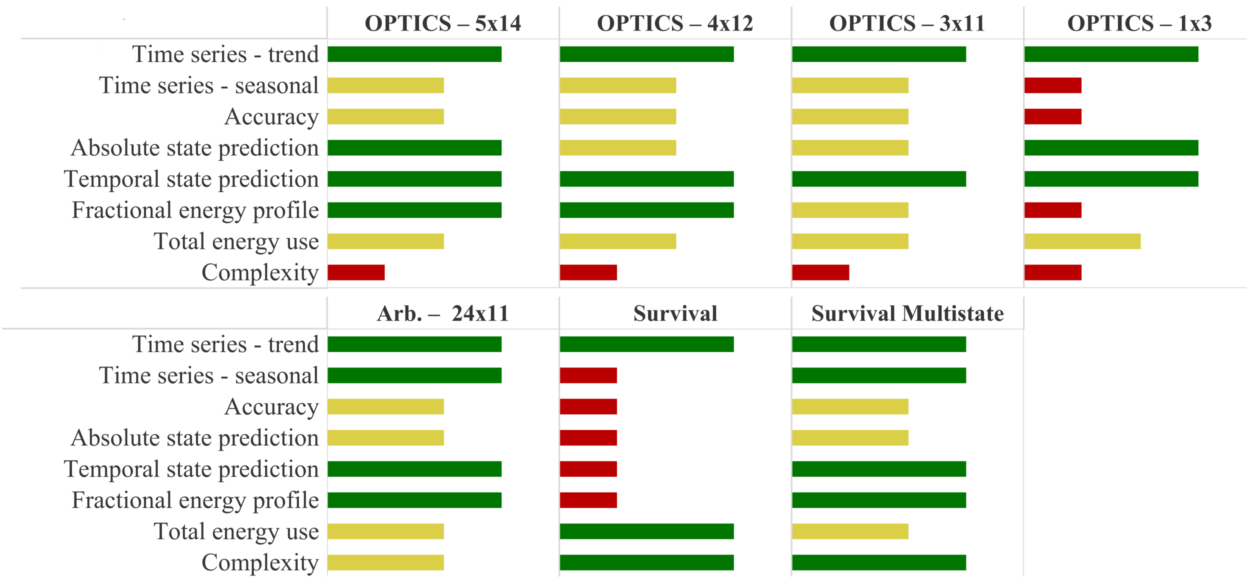

Figure 10: Summary of validation results between the approaches tested, qualitatively represented as *good* (long green bar), *average* (yellow medium bar) and *poor* (short red bar).

4.4. Application of Survival Multistate approach to other categories

In this section results for the simulation of the energy use of computing devices, small kitchen appliances and a category of "other" appliances is presented, following the Survival Multistate approach.

Discussion on modelling a diversity of appliances

Modelling categories of appliances prevents from the analysis of different behaviours from specific devices, which are in a large range of total time of use (between commonly-used and seldom-used appliances) and peak demand values (low-rated and high-rated appliances). At the extremes of this range two types of behaviours have been identified: dominant appliances (commonly-used and high-rated) and infrequent appliances (very rarely used over the course of a year, independently of their rated power). In both cases, these behaviours are undetected by our modelling approach, with corresponding implications for predictive accuracy.

In the case of the kitchen category, preliminary results as described in 2 led to the elimination of the kettle as part of the category. As a high-rated appliance that is commonly owned and used, its behaviour is dominant, misleading the extraction of parameters of the model. Figure 11 shows the results for the survival multistate model applied to the kitchen category with and without the kettle. In this particular case, the total energy use was underestimated by the model, due to its inability to discriminate between the power use pattern of this particular appliance and the other small kitchen appliances. Once removed, the result shows a very good fit with the observed data.

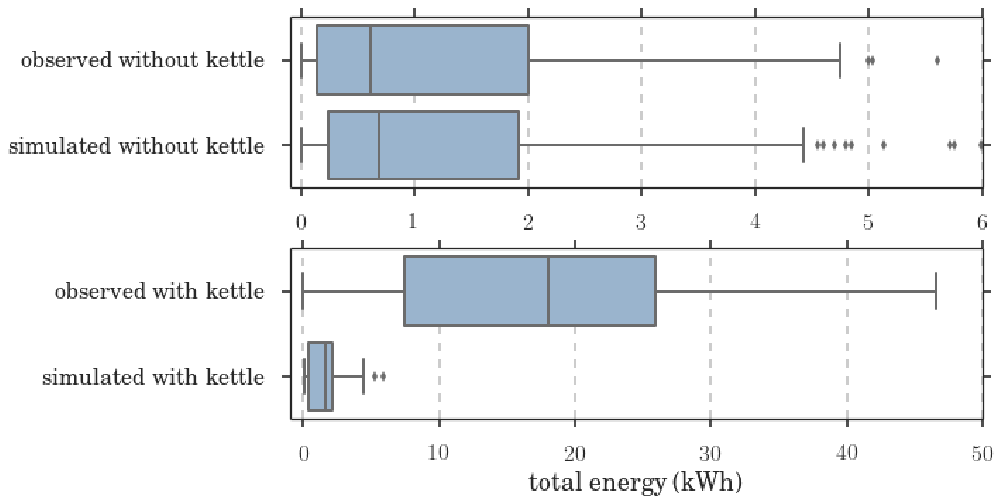

Figure 11: Effect of a dominant appliance (kettle) on the observed and simulated data for the kitchen category.

The category of *other* appliances, on the other hand, is biased by the effect of infrequent appliances, which were monitored in the survey but are very rarely used: several being used only for less than 1% of the total recorded time. Consequently, the total energy use predicted was overestimated.

Performance of the model

The performance of the model has been evaluated in a similar fashion to that for the audio-visual category, and is summarized in table 8. In general, the model performs comparably to that of the modelling of audio-visual appliances. The results are remarkably good for the case of the kitchen devices, once the kettle was removed, proving that the strategy is very powerful for modelling relatively homogeneous type of appliances. Larger errors in energy prediction are found for the other two cases, related again to the diversity of behaviours present on the dataset, as explained in 4.3.3. Notwithstanding this, the average fractional energy use is well predicted, as are the states (table 8).

Error measure		Computing	Kitchen	Other
Time series analysis	Relative error trend	15.7%	0.429%	8, 49%
	Pearson's coefficient	0.967	0.946	0.927
	Lag	-0.014	-0.0005	-0.014
ROC curve	TPR	0.205	0.842	0.783
	TNR	0.920	0.984	0.978
	ACC	0.485	0.517	0.514
Daily profile (RMSE)	Fractional energy (f)	$4.44 \cdot 10^{-2}$	$2.23 \cdot 10^{-3}$	$1.27 \cdot 10^{-2}$
	Absolute state prediction	$5.48 \cdot 10^{-2}$	$6.16 \cdot 10^{-3}$	$1.77 \cdot 10^{-2}$
	Temporal state prediction	$4.08 \cdot 10^{-2}$	$1.06 \cdot 10^{-2}$	$1.70 \cdot 10^{-2}$
Total Energy (kWh)	Mean Residual	-26.4	-0.318	17.7
	Median Residual	-19.0	-0.160	-20.6

Table 8: Summary of results on application of Survival Multistate approach to other categories for: time series analysis, sensitivity and specificity, RMSE of daily profile and total energy.

4.5. Global performance and application of the model

The application of the model is shown in this section in two ways: the first involves a single day simulation for a specific household (labelled in the dataset as "103028"), presented in figure 12. It contains 13 different low-load appliances, which are described in table 9. Figure 12 displays the output of the model, for the four categories, when using the listed appliances. As expected, the model predicts usages of different duration and it is able to capture the spikes in the profiles. But, as expected, the model does not resolve for the specific characteristics of the individual appliances, and it does not represent different behaviours between them. However, the more common usage of audio-visual and computing appliances is well captured.

	Appliance type	**Rated Power (W)**
Audio-visual	Set top box	30
	Audio-visual site	43.2
	DVD/VCR	12.6
Kitchen	Bread maker	97.2
	Toaster	720
	Extractor	16.8
Computing	Laptop	48.6
	Computer equipement	3.6
	Desktop	108
	Monitor	30
	Router	7.2
Other	Housework	1248
	Various	54.6

Table 9: Available appliances in house "103028" and their rated values, extracted from the data set.

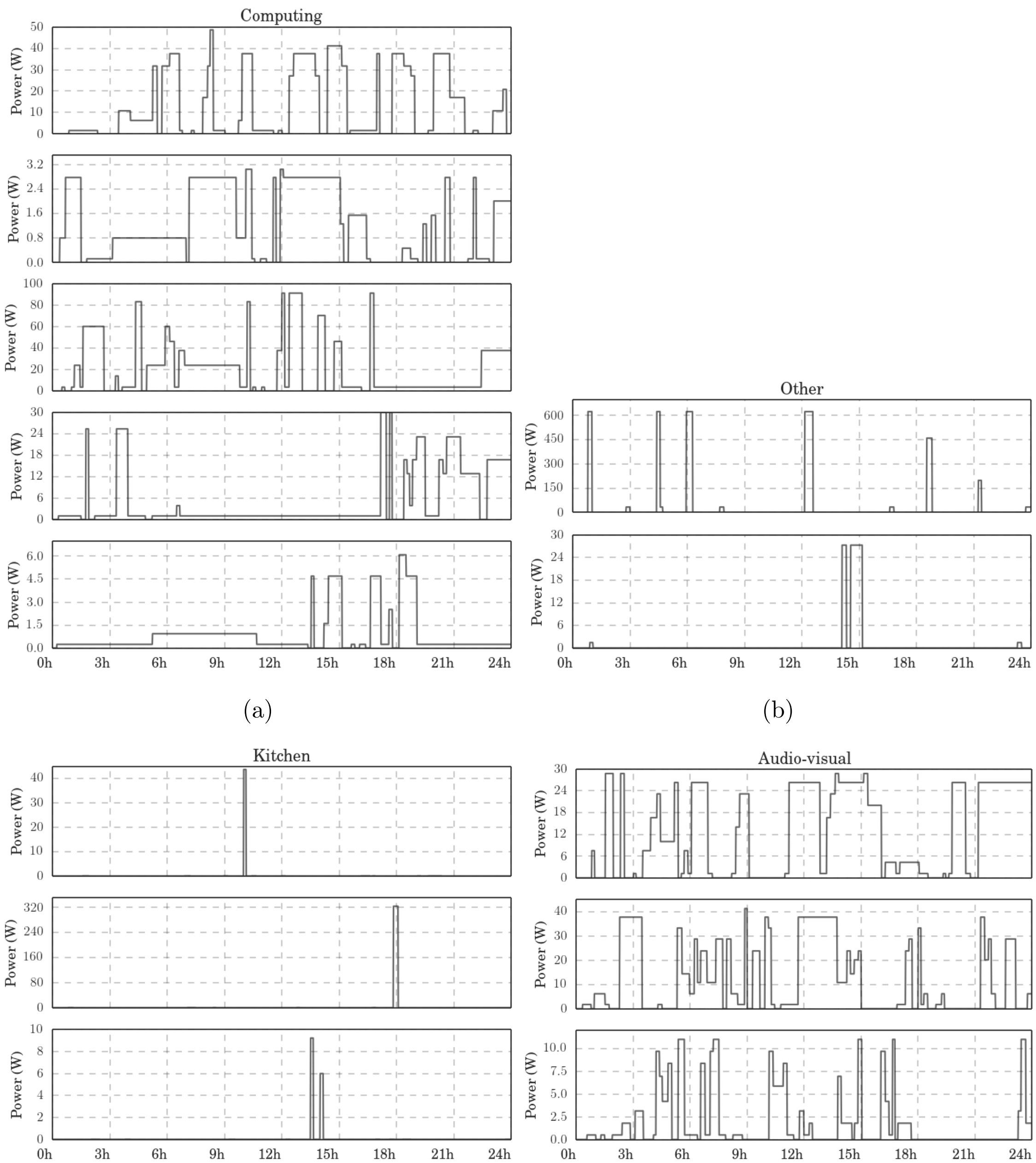

(a) (b)

(c) (d)

Figure 12: Example of one-day simulation for low-load appliances, by category: (a) computing, (b) other, (c) kitchen, (d) audio-visual. They correspond from upper to lower as indicated in table 9.

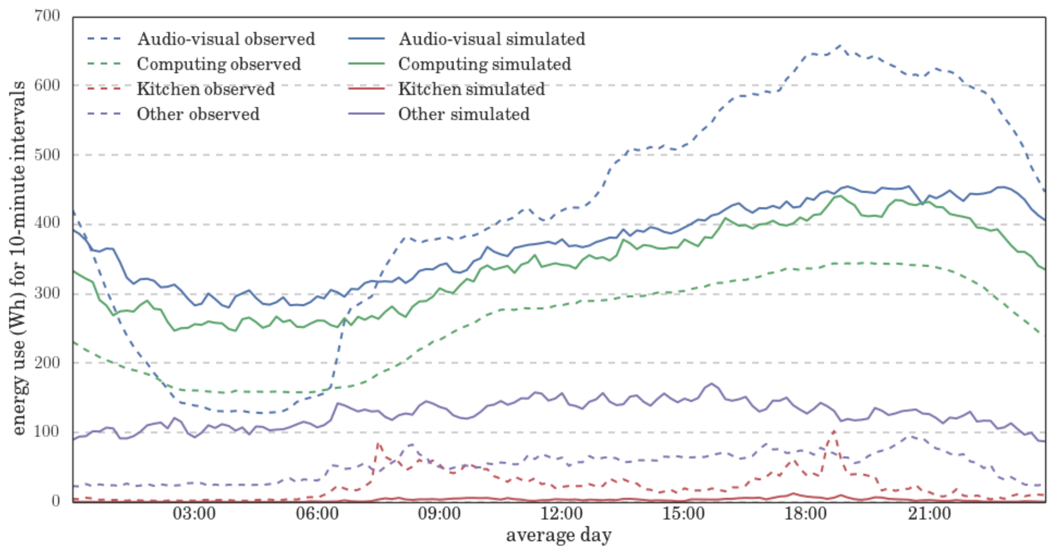

Figure 13: Averaged daily total energy usage from the different categories.

The second includes the averaged daily energy usage arising from all the devices in the different categories of appliances over the year, when aggregated to a community of 20 households (figure 13). This situation is much more representative of the intended usage of the model than for the modelling of individual appliances in a single household. In this case, the total energy use for each category (adding up all the available devices in each household) is averaged in order to create a typical day profile for the community. Then observed and simulated data are compared. Simulated audio-visual appliances describe temporal variability, although its dependency is not as strong as in reality. The use of computing appliances is consistently slightly overestimated, but still captures variations during the day. The use of kitchen devices is slightly underestimated, and the opposite happens with the other category; this could be related to the amount and type of devices of available for this particular group of households, given that their use is reduced. We can conclude that despite of modelling appliances in a generalised way, where devices are not considered individually, realistic magnitudes for the electrical energy use with respect to time can still be obtained.

The parameters used in both cases are those detailed in Appendix A. Profiles for the energy use of the four categories of low-load appliances are thus obtained and compared against the profiles of a selected household.

5. Conclusion

As the integrity of the envelope of both new and existing houses improves, so the proportion of energy that is used by household electrical appliances, which are becoming increasingly ubiquitous, is likely to increase. It is important then that modellers have at their disposal reliable models of appliance energy use, if they are to accurately predict the thermal performance and energy use of future homes. Furthermore, there is increasing interest in the concept of smart grids, to better regulate the distributed supply, storage and demand of electrical energy. This places increasing onus on the ability to predict the dynamic behaviour of household electrical appliances. Whilst good progress has recently been made in the modelling of relatively large appliances: those whose prevalence and cumulative energy use supports the estimation of device-specific models. Poor progress has been made in the modelling of relatively small appliances: those whose cumulative energy use is individually small, but significant when considered as aggregates by typology. To this end we have tested a range of strategies for the modelling of small appliance categories; first predicting discrete states in fractional energy demand, then converting into absolute energy demand, given an estimate of the corresponding maximum power demand.

In this we deploy both discrete (Markov) and continuous (survival) time random processes; and for the former we also deploy cluster analysis to effectively partition the state transition probability space.

From this we draw the following conclusions:

- Modelling appliances by their typologies presents many advantages: it provides a straightforward solution for modelling the range of types of appliances, it reduces the amount of input data needed to estimate the model and the risk of overfitting, and it avoids the time-consuming process of modelling appliances individually, simplifying dynamic energy simulation.

- The model predicting time varying fractional power demands is surprisingly robust, given that it is modelling aggregates. We find that:

- – Finer discretisation of temporal states improved predictive power, but these improvements are modest beyond 5 temporal states.
  – Appropriate estimation of the number of fractional energy states is not as influential as the number of temporal states.

- Clustering techniques have been effectively deployed to objectively search for a parsimonious form of model: minimising the size and number of state transition probability matrices. The methods presented can be used for many other areas of research.

- Based on three types of evaluation measure (time series analysis, model accuracy and aggregated energy use), the survival multistate approach, in which survival times are estimated for selected bins of fractional energy demand, clearly outperforms its Markov process counterparts.

- However, analysing categories can compromise the fidelity of predictions of aggregate energy use, particularly if modelling small numbers of households. In our case, a successful strategy consisted of allocating maximum energy values with a random assignment process. The survival multistate approach has been effectively deployed to model low-load appliances in four categories: audio-visual, computing kitchen and other. The profiles output by the model have been satisfactorily compared to those of a community of households.

This work forms part of a larger programme of research to reliably predict appliance energy demand using bottom-up techniques for communities of households, and to test strategies for the management of these appliance demands to improve community energy autonomy. The testing and evaluation of these Demand Side Management strategies will be reported in a future paper.

Acknowledgements

Authors gratefully acknowledge the European Commission for providing financial support during the conduct of research under FP7-PEOPLE-2013 Marie Curie Initial Training Network "CI-NERGY" project with Grant Agreement Number 606851.

References

[1] Department of Energy and Climate Change. Energy consumption in the UK (2015). Technical report.

[2] S. Jaboob. *On the ownership and use of residential electrical appliances*. PhD thesis, University of Nottingham, 2015.

[3] A. Sancho Tomás, M. Sumner, S. Lamparter, and D. Robinson. On the energy demands of small appliances in homes. *Energy Procedia*, 78:3384 – 3390, 2015. 6th International Building Physics Conference, IBPC 2015.

[4] A. Grandjean, J. Adnot, and G. Binet. A review and an analysis of the residential electric load curve models. *Renewable and Sustainable Energy Reviews*, 16(9):6539–6565, 2012.

[5] M. Stokes. *Removing barriers to embedded generation: a fine-grained load model to support low voltage network performance analysis*. PhD thesis, De Montfort University, Leicester, UK, 2005.

[6] J. V. Paatero and P. D. Lund. A model for generating household electricity load profiles. *International Journal of Energy Research*, 30(5):273–290, April 2006.

[7] A. Capasso, W. Grattieri, R. Lamedica, and a. Prudenzi. A bottom-up approach to residential load modeling. *IEEE Transactions on Power Systems*, 9(2):957–964, May 1994.

[8] J. Tanimoto, A. Hagishima, and H. Sagara. Validation of probabilistic methodology for generating actual inhabitants' behavior schedules for accurate prediction of maximum energy requirements. *Energy and Buildings*, 40(3):316–322, January 2008.

[9] J. Widén, M. Lundh, I. Vassileva, E. Dahlquist, K. Ellegård, and E. Wäckelgård. Constructing load profiles for household electricity and hot water from time-use data-modelling approach and validation. *Energy and Buildings*, 41(7-1):753 – 768, July 2009.

[10] J. Widén and E. Wäckelgård. A high-resolution stochastic model of domestic activity patterns and electricity demand. *Applied Energy*, 87(6):1880–1892, June 2010.

[11] I. Richardson, M. Thomson, D. Infield, and C. Clifford. Domestic electricity use: A high-resolution energy demand model. *Energy and Buildings*, 42(10):1878–1887, October 2010.

[12] J. Page, D. Robinson, N. Morel, and J.-L. Scartezzini. A generalised stochastic model for the simulation of occupant presence. *Energy and Buildings*, 40(2):83–98, January 2008.

[13] F. Haldi and D. Robinson. Adaptive actions on shading devices in response to local visual stimuli. *Journal of Building Performance Simulation*, 3(2):135–153, June 2010.

[14] F. Haldi and D. Robinson. Interactions with window openings by office occupants. *Building and Environment*, 44(12):2378–2395, December 2009.

[15] A. T. Bharucha-Reid. *Elements of the Theory of Markov Processes and their Applications*. Courier Corporation, North Chelmsford , MA (US), 2012.

[16] A. K. Jain, M. N. Murty, and P. J. Flynn. Data clustering: A review. *ACM Computing Surveys*, 31(3):264–323, September 1999.

[17] M. Ankerst, M. M. Breunig, H.-P. Kriegel, and J. Sander. OPTICS: Ordering points to identify the clustering structure. In *Proceedings of the 1999 ACM SIGMOD International Conference on Management of Data*, SIGMOD '99, pages 49–60, New York, NY, USA, 1999. ACM.

[18] M. Ester, H.-P. Kriegel, J. Sander, and X. Xu. A density-based algorithm for discovering clusters in large spatial databases with noise. In *Proceedings of 2nd International Conference on Knowledge Discovery and Data Mining*, volume 96, pages 226–231, 1996.

[19] J. Sander, X. Qin, Z. Lu, N. Niu, and A. Kovarsky. Automatic extraction of clusters from hierarchical clustering representations. In *Advances in Knowledge Discovery and Data Mining*, volume 2637 of *Lecture Notes in Computer Science*, pages 75–87. Springer Berlin Heidelberg, 2003.

[20] D. R. Cox and D. Oakes. *Analysis of survival data*, volume 21. CRC Press, Boca Raton, USA, 1984.

[21] Department of Energy and Climate Change and Intertek Testing and Certification Ltd. Household Electricity Survey.

[22] O. Vallis, J. Hochenbaum, and A. Kejariwal. A novel technique for long-term anomaly detection in the cloud. In *6th USENIX Workshop on Hot Topics in Cloud Computing (HotCloud 14)*, Philadelphia, PA, June 2014. USENIX Association.

[23] R Core Team. *R: A Language and Environment for Statistical Computing*. R Foundation for Statistical Computing, Vienna, Austria, 2015.

[24] R. Kohavi. A study of cross-validation and bootstrap for accuracy estimation and model selection. In *Proceedings of the 14th International Joint Conference on Artificial Intelligence - Volume 2*, IJCAI'95, pages 1137–1143, San Francisco, CA, USA, 1995. Morgan Kaufmann Publishers Inc.

[25] G.E.P. Box and G. M. Jenkins. *Time series analysis: forecasting and control.* John Wiley & Sons, Hoboken, New Jersey, 2015.

[26] Chao-Ying Joanne Peng and Tak-Shing Harry So. Logistic regression analysis and reporting: A primer. *Understanding Statistics: Statistical Issues in Psychology, Education, and the Social Sciences*, 1(1):31–70, 2002.

[27] D.S. Starnes, J. Tabor, D. Yates, and D.S. Moore. *The Practice of Statistics.* W. H. Freeman, 2014.

Appendix A.

For purposes of implementation of the model, tables 10, 11, 12, 13 and 14 contain the values of the parameters obtained from the dataset. The survival multistate model is presented in Algorithm 1 as pseudo-code.

Algorithm 1 Simulate Small Appliance Usage ($([\lambda, k, \gamma]_{\mathbf{s}}$, P(t,**s**)$)$)

$s = 0$ ▷ Asume initial state s_0.
$t = t_{START}$
while $t < t_{END}$ **do**
  % Calculate duration at state s
  $R1 = random(0, 1)$
  $\lambda, k, \gamma = \lambda_s, k_s, \gamma_s$ ▷ Use table 10.
  $t_s = \gamma + \lambda \left[-\ln(R1)\right]^{1/k}$
  $t = t + t_s$
  % Calculate next state
  $R2 = random(0, 1)$
  $s = MinIdx\left[(cdf\,P(t) - R2) > 0\right]$ ▷ Use table table 12 and 13.
  Append s to s_{arr}
end while
%Transform into fractional energy array.
$f_{arr} = \tilde{F}_s \times s_{arr}$ ▷ Use table 11.
%Transform into energy use array.
$E_{arr} = \tilde{E}_{max} \times f_{arr}$ ▷ Use table 14.

Energy state	Audio-visual			Computing			Kitchen			Other		
	γ	k	λ	γ	k	λ	γ	k	λ	γ	k	λ
s_0	8.92	0.743	10.74	7.52	1.529	12.52	7.80	1.37	4.29	7.46	0.930	9.61
s_1	8.29	0.916	7.52	7.29	1.110	4.87	8.93	1.17	6.57	8.25	1.148	5.20
s_2	8.38	1.096	9.82	8.03	0.889	5.37	8.39	1.25	4.29	8.83	1.147	7.16
s_3	8.33	0.965	6.95	8.83	0.607	20.14	8.13	1.06	5.35	9.34	1.201	9.03
s_4	8.95	0.648	12.20	8.52	0.977	6.19	8.02	1.26	4.50	8.86	0.872	7.34
s_5	9.45	0.980	15.59	8.13	0.870	6.36	8.34	1.27	4.20	9.03	1.148	13.35
s_6	9.02	0.747	13.06	8.68	0.790	7.76	8.72	1.12	5.21	8.89	1.070	6.92
s_7	9.03	1.065	11.72	8.76	0.854	10.97	8.22	1.33	4.01	8.23	1.046	5.32
s_8	8.40	1.005	7.25	8.95	0.657	13.82	7.63	1.28	4.58	8.39	1.214	4.47
s_9	8.79	0.805	13.93	8.70	0.872	15.63	8.01	1.24	4.36	8.64	0.989	6.30
s_{10}	8.24	1.051	5.56	8.30	1.093	5.72	8.73	1.16	7.12	8.65	0.963	8.62

Table 10: Survival distribution parameters (γ: location, k: shape, λ: scale) for four categories.

Energy state	$\tilde{F}_{Audio-visual}$	$\tilde{F}_{Computing}$	$\tilde{F}_{Kitchen}$	$\tilde{F}_{Other}$
s_0	0.0000	0.0000	0.0000	0.0000
s_1	0.0402	0.0333	0.0007	0.0265
s_2	0.1429	0.1297	0.1382	0.1587
s_3	0.2500	0.2222	0.2473	0.2513
s_4	0.3333	0.3500	0.3570	0.3684
s_5	0.4667	0.4286	0.4494	0.5000
s_6	0.5525	0.5581	0.5495	0.5450
s_7	0.6660	0.6526	0.6597	0.6565
s_8	0.7708	0.7717	0.7463	0.7500
s_9	0.8750	0.8462	0.8405	0.8333
s_{10}	0.9571	1.0000	0.9684	0.9167

Table 11: Median fractional energy for transforming energy states into fractional energy profiles.

Hour of day	Audio-visual										
	$P(s=s_0)$	$P(s=s_1)$	$P(s=s_2)$	$P(s=s_3)$	$P(s=s_4)$	$P(s=s_5)$	$P(s=s_6)$	$P(s=s_7)$	$P(s=s_8)$	$P(s=s_9)$	$P(s=s_{10})$
0h	0.3587	0.1437	0.1174	0.0792	0.0406	0.0392	0.0293	0.0443	0.0470	0.0710	0.0295
1h	0.3799	0.1566	0.1172	0.0800	0.0353	0.0378	0.0305	0.0446	0.0459	0.0517	0.0205
2h	0.3844	0.1667	0.1171	0.0803	0.0332	0.0372	0.0384	0.0423	0.0442	0.0408	0.0153
3h	0.3859	0.1715	0.1157	0.0820	0.0302	0.0375	0.0441	0.0403	0.0441	0.0366	0.0122
4h	0.3883	0.1756	0.1128	0.0813	0.0298	0.0398	0.0440	0.0400	0.0436	0.0336	0.0113
5h	0.3879	0.1797	0.1088	0.0805	0.0298	0.0398	0.0448	0.0412	0.0420	0.0342	0.0114
6h	0.3853	0.1719	0.1115	0.0785	0.0303	0.0379	0.0419	0.0424	0.0449	0.0404	0.0151
7h	0.3781	0.1638	0.1117	0.0799	0.0336	0.0391	0.0456	0.0404	0.0451	0.0436	0.0193
8h	0.3607	0.1704	0.1020	0.0805	0.0368	0.0412	0.0506	0.0412	0.0460	0.0481	0.0223
9h	0.3437	0.1709	0.1029	0.0845	0.0390	0.0423	0.0509	0.0427	0.0481	0.0499	0.0251
10h	0.3311	0.1682	0.1057	0.0860	0.0397	0.0438	0.0521	0.0426	0.0475	0.0542	0.0291
11h	0.3283	0.1657	0.1044	0.0859	0.0377	0.0419	0.0518	0.0414	0.0502	0.0595	0.0333
12h	0.3287	0.1610	0.1022	0.0876	0.0332	0.0413	0.0502	0.0410	0.0542	0.0648	0.0358
13h	0.3255	0.1554	0.1032	0.0872	0.0318	0.0434	0.0485	0.0400	0.0549	0.0701	0.0400
14h	0.3202	0.1540	0.1049	0.0860	0.0322	0.0436	0.0467	0.0417	0.0567	0.0718	0.0421
15h	0.3144	0.1496	0.1027	0.0865	0.0346	0.0480	0.0441	0.0465	0.0566	0.0730	0.0440
16h	0.3073	0.1408	0.1035	0.0879	0.0374	0.0505	0.0426	0.0494	0.0560	0.0753	0.0492
17h	0.3021	0.1319	0.1039	0.0905	0.0387	0.0512	0.0443	0.0515	0.0564	0.0786	0.0510
18h	0.2994	0.1280	0.1020	0.0888	0.0399	0.0497	0.0454	0.0539	0.0565	0.0825	0.0539
19h	0.3001	0.1267	0.1022	0.0892	0.0416	0.0518	0.0417	0.0500	0.0563	0.0880	0.0523
20h	0.2976	0.1279	0.1068	0.0902	0.0425	0.0471	0.0400	0.0492	0.0555	0.0887	0.0545
21h	0.2953	0.1276	0.1054	0.0904	0.0438	0.0461	0.0409	0.0470	0.0565	0.0921	0.0550
22h	0.3008	0.1289	0.1046	0.0854	0.0450	0.0475	0.0418	0.0458	0.0550	0.0933	0.0519
23h	0.3222	0.1340	0.1097	0.0817	0.0449	0.0457	0.0383	0.0450	0.0512	0.0862	0.0411

Hour of day	Computing										
	$P(s=s_0)$	$P(s=s_1)$	$P(s=s_2)$	$P(s=s_3)$	$P(s=s_4)$	$P(s=s_5)$	$P(s=s_6)$	$P(s=s_7)$	$P(s=s_8)$	$P(s=s_9)$	$P(s=s_{10})$
0h	0.4084	0.2563	0.0450	0.0370	0.0266	0.0376	0.0405	0.0410	0.0534	0.0394	0.0148
1h	0.4232	0.2626	0.0479	0.0373	0.0237	0.0341	0.0349	0.0348	0.0520	0.0361	0.0134
2h	0.4306	0.2672	0.0544	0.0382	0.0229	0.0326	0.0273	0.0324	0.0496	0.0325	0.0124
3h	0.4348	0.2679	0.0575	0.0379	0.0225	0.0322	0.0237	0.0307	0.0480	0.0325	0.0122
4h	0.4361	0.2676	0.0578	0.0379	0.0226	0.0317	0.0240	0.0300	0.0388	0.0411	0.0123
5h	0.4364	0.2664	0.0575	0.0379	0.0230	0.0319	0.0238	0.0334	0.0474	0.0311	0.0113
6h	0.4331	0.2653	0.0565	0.0376	0.0234	0.0324	0.0257	0.0373	0.0486	0.0296	0.0105
7h	0.4259	0.2589	0.0526	0.0376	0.0247	0.0334	0.0323	0.0428	0.0499	0.0307	0.0113
8h	0.4138	0.2484	0.0461	0.0379	0.0265	0.0352	0.0409	0.0514	0.0544	0.0333	0.0122
9h	0.4001	0.2394	0.0432	0.0382	0.0303	0.0357	0.0445	0.0563	0.0607	0.0376	0.0141
10h	0.3884	0.2328	0.0417	0.0391	0.0322	0.0376	0.0487	0.0589	0.0627	0.0419	0.0161
11h	0.3818	0.2295	0.0405	0.0381	0.0322	0.0403	0.0517	0.0603	0.0629	0.0447	0.0181
12h	0.3773	0.2268	0.0389	0.0392	0.0327	0.0407	0.0539	0.0614	0.0642	0.0458	0.0191
13h	0.3723	0.2259	0.0376	0.0397	0.0327	0.0425	0.0548	0.0621	0.0642	0.0482	0.0201
14h	0.3660	0.2249	0.0376	0.0403	0.0329	0.0428	0.0558	0.0636	0.0655	0.0493	0.0214
15h	0.3548	0.2228	0.0376	0.0407	0.0340	0.0436	0.0559	0.0663	0.0691	0.0524	0.0227
16h	0.3428	0.2223	0.0375	0.0409	0.0367	0.0411	0.0587	0.0675	0.0719	0.0555	0.0251
17h	0.3336	0.2179	0.0386	0.0411	0.0385	0.0417	0.0604	0.0700	0.0736	0.0579	0.0266
18h	0.3252	0.2141	0.0396	0.0411	0.0394	0.0451	0.0619	0.0708	0.0765	0.0600	0.0263
19h	0.3196	0.2118	0.0395	0.0430	0.0380	0.0495	0.0633	0.0706	0.0784	0.0599	0.0266
20h	0.3162	0.2156	0.0391	0.0439	0.0384	0.0511	0.0627	0.0683	0.0775	0.0602	0.0270
21h	0.3192	0.2213	0.0391	0.0426	0.0359	0.0536	0.0615	0.0674	0.0732	0.0585	0.0276
22h	0.3430	0.2349	0.0413	0.0403	0.0310	0.0490	0.0555	0.0622	0.0666	0.0512	0.0250
23h	0.3785	0.2498	0.0433	0.0366	0.0286	0.0434	0.0469	0.0519	0.0581	0.0434	0.0195

Table 12: Hourly state probability for Audio-visual and Computing categories.

Hour of day	Kitchen										
	$P(s=s_0)$	$P(s=s_1)$	$P(s=s_2)$	$P(s=s_3)$	$P(s=s_4)$	$P(s=s_5)$	$P(s=s_6)$	$P(s=s_7)$	$P(s=s_8)$	$P(s=s_9)$	$P(s=s_{10})$
0h	0.9403	0.0567	0.0006	0.0007	0.0006	0.0005	0.0004	0.0002	0.0000	0.0000	0.0000
1h	0.9418	0.0561	0.0003	0.0004	0.0005	0.0004	0.0003	0.0001	0.0001	0.0001	0.0000
2h	0.9408	0.0560	0.0004	0.0005	0.0007	0.0007	0.0005	0.0002	0.0001	0.0000	0.0000
3h	0.9357	0.0580	0.0008	0.0009	0.0017	0.0016	0.0008	0.0003	0.0001	0.0001	0.0001
4h	0.9328	0.0595	0.0016	0.0012	0.0022	0.0017	0.0004	0.0003	0.0002	0.0002	0.0001
5h	0.9209	0.0624	0.0033	0.0025	0.0049	0.0034	0.0017	0.0005	0.0002	0.0001	0.0001
6h	0.9041	0.0719	0.0061	0.0034	0.0054	0.0048	0.0026	0.0010	0.0003	0.0002	0.0001
7h	0.8768	0.0836	0.0090	0.0068	0.0086	0.0079	0.0038	0.0023	0.0007	0.0004	0.0001
8h	0.8683	0.0862	0.0114	0.0084	0.0100	0.0081	0.0047	0.0015	0.0006	0.0005	0.0004
9h	0.8656	0.0924	0.0096	0.0082	0.0084	0.0073	0.0041	0.0023	0.0009	0.0008	0.0004
10h	0.8740	0.0913	0.0077	0.0077	0.0072	0.0057	0.0030	0.0015	0.0006	0.0007	0.0005
11h	0.8759	0.0910	0.0069	0.0075	0.0075	0.0056	0.0028	0.0013	0.0006	0.0005	0.0004
12h	0.8854	0.0861	0.0056	0.0068	0.0070	0.0045	0.0026	0.0010	0.0005	0.0003	0.0002
13h	0.8822	0.0870	0.0056	0.0076	0.0076	0.0048	0.0028	0.0013	0.0006	0.0004	0.0002
14h	0.8839	0.0879	0.0053	0.0076	0.0072	0.0040	0.0022	0.0010	0.0004	0.0004	0.0002
15h	0.8858	0.0847	0.0056	0.0073	0.0077	0.0045	0.0021	0.0010	0.0005	0.0004	0.0004
16h	0.8863	0.0839	0.0058	0.0069	0.0066	0.0046	0.0029	0.0012	0.0011	0.0005	0.0003
17h	0.8839	0.0845	0.0062	0.0077	0.0065	0.0043	0.0025	0.0014	0.0017	0.0005	0.0007
18h	0.8932	0.0792	0.0055	0.0063	0.0059	0.0043	0.0021	0.0012	0.0012	0.0006	0.0004
19h	0.9016	0.0760	0.0045	0.0053	0.0049	0.0035	0.0020	0.0010	0.0006	0.0004	0.0002
20h	0.9072	0.0719	0.0039	0.0048	0.0052	0.0036	0.0015	0.0009	0.0005	0.0003	0.0002
21h	0.9171	0.0672	0.0026	0.0037	0.0044	0.0024	0.0012	0.0007	0.0004	0.0001	0.0002
22h	0.9248	0.0634	0.0021	0.0033	0.0030	0.0017	0.0008	0.0005	0.0002	0.0001	0.0000
23h	0.9323	0.0605	0.0017	0.0021	0.0012	0.0010	0.0006	0.0003	0.0001	0.0000	0.0001

Hour of day	Other										
	$P(s=s_0)$	$P(s=s_1)$	$P(s=s_2)$	$P(s=s_3)$	$P(s=s_4)$	$P(s=s_5)$	$P(s=s_6)$	$P(s=s_7)$	$P(s=s_8)$	$P(s=s_9)$	$P(s=s_{10})$
0h	0.8724	0.0841	0.0012	0.0029	0.0097	0.0182	0.0001	0.0000	0.0112	0.0000	0.0001
1h	0.8730	0.0835	0.0013	0.0027	0.0096	0.0200	0.0000	0.0000	0.0097	0.0000	0.0000
2h	0.8722	0.0830	0.0013	0.0026	0.0101	0.0201	0.0001	0.0000	0.0105	0.0000	0.0001
3h	0.8720	0.0821	0.0014	0.0025	0.0098	0.0212	0.0002	0.0000	0.0107	0.0000	0.0001
4h	0.8725	0.0817	0.0013	0.0026	0.0097	0.0219	0.0002	0.0000	0.0101	0.0000	0.0001
5h	0.8718	0.0788	0.0015	0.0027	0.0109	0.0245	0.0004	0.0001	0.0092	0.0000	0.0001
6h	0.8692	0.0765	0.0022	0.0032	0.0120	0.0284	0.0004	0.0002	0.0077	0.0000	0.0001
7h	0.8674	0.0757	0.0026	0.0036	0.0127	0.0301	0.0008	0.0003	0.0066	0.0001	0.0001
8h	0.8644	0.0731	0.0029	0.0038	0.0136	0.0331	0.0011	0.0005	0.0069	0.0003	0.0003
9h	0.8631	0.0741	0.0026	0.0036	0.0141	0.0329	0.0010	0.0007	0.0071	0.0004	0.0004
10h	0.8577	0.0743	0.0034	0.0044	0.0143	0.0335	0.0015	0.0014	0.0084	0.0008	0.0003
11h	0.8556	0.0737	0.0040	0.0046	0.0149	0.0347	0.0013	0.0015	0.0086	0.0008	0.0003
12h	0.8571	0.0729	0.0038	0.0044	0.0146	0.0342	0.0014	0.0012	0.0089	0.0013	0.0003
13h	0.8565	0.0744	0.0037	0.0039	0.0154	0.0334	0.0013	0.0015	0.0085	0.0011	0.0003
14h	0.8579	0.0654	0.0130	0.0031	0.0151	0.0322	0.0015	0.0011	0.0094	0.0011	0.0003
15h	0.8600	0.0596	0.0197	0.0020	0.0143	0.0321	0.0019	0.0011	0.0084	0.0006	0.0002
16h	0.8614	0.0622	0.0199	0.0022	0.0136	0.0293	0.0015	0.0007	0.0073	0.0007	0.0011
17h	0.8615	0.0642	0.0198	0.0022	0.0131	0.0278	0.0015	0.0007	0.0070	0.0010	0.0010
18h	0.8622	0.0659	0.0201	0.0024	0.0126	0.0254	0.0014	0.0005	0.0074	0.0011	0.0010
19h	0.8639	0.0664	0.0204	0.0016	0.0125	0.0242	0.0011	0.0005	0.0075	0.0008	0.0012
20h	0.8639	0.0658	0.0203	0.0018	0.0127	0.0246	0.0010	0.0005	0.0075	0.0006	0.0013
21h	0.8639	0.0681	0.0195	0.0020	0.0111	0.0220	0.0009	0.0003	0.0092	0.0007	0.0022
22h	0.8624	0.0804	0.0088	0.0031	0.0103	0.0192	0.0007	0.0003	0.0114	0.0003	0.0030
23h	0.8701	0.0847	0.0018	0.0032	0.0098	0.0177	0.0002	0.0001	0.0119	0.0001	0.0003

Table 13: Hourly state probability for Kitchen and Other categories.

Audio-visual	Computing	Kitchen	Other
1.8	0.0	0.0	0.0
18.0	0.0	0.0	0.0
27.0	0.0	0.0	0.0
30.0	0.0	0.0	0.0
43.2	6.0	0.0	0.0
50.4	58.8	0.0	0.0
54.0	63.0	0.0	0.0
85.8	99.0	0.0	0.0
97.2	105.0	0.0	0.0
98.4	135.0	0.0	0.0
145.2	138.0	0.0	0.0
148.8	139.2	0.0	0.0
153.6	143.4	9.6	0.0
210.0	150.0	91.8	0.0
297.6	151.2	258.0	0.0
312.6	156.6	267.6	0.0
430.8	197.4	580.8	0.0
459.0	228.6	580.8	2.4
518.4	417.0	691.2	30.0
657.0	424.2	723.0	45.6
754.2	628.8	834.0	241.2
892.2	816.6	1416.0	915.0
1037.4	1119.6	1662.6	1213.8
1499.4	1495.8	1755.6	2861.4
2035.2	2625.0	2850.0	3811.8

Table 14: Sum of rated power (W) for all the corresponding low-load appliances in each household, for the 26 houses considered in the dataset. Cases where power is 0.0W are households with devices that have been removed from the modelling (for reasons specified in the text) or household that do not own any of these appliances.